

Contents lists available at ScienceDirect

# Transportation Research Part C

journal homepage: www.elsevier.com/locate/trc



# Smoothing-MP: A novel max-pressure signal control considering signal coordination to smooth traffic in urban networks

Te Xu<sup>a,b,\*</sup>, Simanta Barman a,b,c, Michael W. Levin a

- <sup>a</sup> Department of Civil, Environmental, and Geo- Engineering, University of Minnesota, Minneapolis, MN, USA
- <sup>b</sup> Department of Industrial and Systems Engineering, University of Minnesota, Minneapolis, MN, USA
- <sup>c</sup> Department of Computer Science and Engineering, University of Minnesota, Minneapolis, MN, USA

#### ARTICLE INFO

# Keywords: Max-pressure signal control Traffic signal coordination Coordinated corridors

### ABSTRACT

Decentralized traffic signal control methods, such as max-pressure (MP) control or back-pressure (BP) control, have gained increasing attention in recent years. MP control, in particular, boasts mathematically-proven network throughput properties, enabling it to optimize network throughput and stabilize vehicle queue lengths whenever possible. Urban traffic volume is dynamic and features a non-uniform distribution throughout the network. Specifically, heavier traffic is often observed along arterial corridors or major origin-destination streams, such as those in central business districts (CBD), while less traffic is found on sub-arterial roads. To address these issues, many existing signal plans incorporate coordinated signal timing. Numerous previous studies have formulated signal coordination optimization as mixed-integer programming problems, with most belonging to centralized traffic signal controller categories. However, centralized approaches do not scale well to larger city networks. In this paper, we introduce a novel max-pressure signal control approach called Smoothing-MP, which considers signal coordination in urban networks to achieve both maximum vehicle stability and reduced travel time and delay along specific urban corridors, without altering the original stable region proposed by Varaiya (2013). This study represents a pioneering effort in modifying max-pressure control to incorporate signal coordination. Crucially, this policy retains the decentralized characteristic of the original max-pressure control, relying exclusively on local information sourced from upstream and downstream intersections. To evaluate the proposed Smoothing-MP control, we executed simulation studies on two different types of networks, the Downtown Austin Network and a Grid Network. The results unequivocally show that Smoothing-MP matches the maximum throughput of the original MP control. Moreover, it significantly reduces both travel time and delay along coordinated corridors. This dual accomplishment underscores the efficacy and potential advantages of the Smoothing-MP control approach.

#### 1. Introduction

Traffic signal lights have been in use for over 100 years since the first colored traffic light was introduced in England in the 19th century (Webster, 1958). The goals of installing traffic signal controls include providing orderly vehicle movements, reducing conflicts, increasing traffic capacity at intersections, assigning right-of-way to increase driver confidence, reducing congestion, and more. Currently, there are two main types of traffic signal controllers widely used in cities. The first is fixed-time control, which requires historical traffic information to create signal timing plans. The other is actuated or adaptive signal controllers, which

https://doi.org/10.1016/j.trc.2024.104760

<sup>\*</sup> Corresponding author at: Department of Civil, Environmental, and Geo- Engineering, University of Minnesota, Minneapolis, MN, USA. *E-mail address*: te000002@umn.edu (T. Xu).

rely on sensors such as loop detectors and video detectors. However, as traffic volumes increase, traffic systems require more advanced traffic signal controllers, particularly network-level traffic signal controllers for urban traffic networks. Most existing traffic signal controllers are centralized, meaning that signals across a network are controlled together. A consequence of that approach is that the computation time increase drastically as the network size increases. Therefore, traffic signal researchers have begun to focus on decentralized traffic signal controllers. Max-pressure (MP) control, also known as back-pressure (BP) control, is one such decentralized traffic signal control policy that has gained attention since (Varaiya, 2013) first proposed it for traffic signal control. It is worth noting that Tassiulas and Ephremides (1990) initially proposed the MP policy in communication and power systems before (Varaiya, 2013) introduced it into traffic signal control. MP control has two main advantages: provable maximum throughput for demand that can be served by any other signal control, and a well-designed decentralized structure. This means that MP control's decision-making relies only on information from upstream and downstream, allowing for excellent scalability.

Traffic patterns are not uniformly distributed throughout city networks. For example, in New York City, the most congested street is the Brooklyn-Queens Expressway, which experiences more daily congestion than other roads. Urban and traffic planners recognize that arterial corridors attract a significant portion of traffic demand in urban areas due to mixed land-use development, which includes business centers, parking lots, shopping malls, and sports and recreational areas. Therefore, arterial corridors require proper signal timing to reduce the number of stops and vehicle delays, providing smooth operation for vehicles traveling through these corridors. Traffic operational efficiency is vital for arterial corridors. Along arterial corridors, numerous continuous signalized intersections exist. If traffic lights can coordinate with one another to provide continuous green lights for vehicles traveling at appropriate speeds, the average number of stops and delays can be significantly reduced. This concept is called signal coordination (Feng., 2015).

Numerous previous research papers have demonstrated that traffic systems can benefit from proper signal coordination design strategies (Ma et al., 2018b; Yao et al., 2019; Yue, 2020). National Academies of Sciences, Engineering, and Medicine et al. (2015) stated that the purpose of coordinating traffic signals is to facilitate smooth traffic flow along streets and highways, ultimately reducing travel times, stops, and delays. In recent decades, the field of signal coordination has evolved significantly, moving beyond traditional methods to more sophisticated approaches. Early systems, such as MAXBAND, proposed by Little et al. (1981), played a foundational role in optimizing bandwidth along arterial corridors. However, these methods, including TRANSYT (Traffic Network Study Tools), faced limitations in complex traffic scenarios, as noted in studies like (Zhang et al., 2016; Arsava et al., 2018; Ma et al., 2018b; Zhang et al., 2015). To address these challenges, researchers have introduced advanced methods. For instance, MULTIBAND by Gartner et al. (1991) and AM-BAND by Zhang et al. (2015) offered more adaptable bandwidth coordination, while PM-BAND by Ma et al. (2018b) and OD-NETBAND by Arsava et al. (2018) integrated specific traffic elements like transit vehicles and major origin–destination flows. Despite these advancements, most research has remained focused on single arterial corridors. There is a growing recognition, as highlighted by Yan et al. (2019) and Zhang et al. (2016), of the need to expand signal coordination to network and area-wide levels. This shift is crucial, especially since existing policies, often framed as mixed-integer programs, lack scalability for larger city networks.

The MP control, a well-designed decentralized signal controller with provable maximum throughput, has attracted our attention. However, it has some limitations, such as activating signals in an arbitrary order (Levin et al., 2020). Some researchers have attempted to enhance the original MP control by designing a cyclic structure, as seen in papers such as (Le et al., 2015; Levin et al., 2020). Other studies suggest that travel time or travel delay-based pressure calculations are more accurate and easier to implement in practical situations than the original queue-length based pressure calculation (Mercader et al., 2020; Liu and Gayah, 2022). MP control was modified for transit signal priority (Xu et al., 2022a) and pedestrian access (Xu et al., 2024a). However, no research has yet integrated both MP control and signal coordination. It is important to note that MP control also falls under the category of actuated or adaptive signal control, as it relies on traffic sensors installed on upstream and downstream roads. Furthermore, Das et al. (2022) indicates that coordination can be integrated with both fixed-time and actuated traffic signal control. Actuated coordination offers more advantages compared to fixed-time coordination due to its ability to respond to dynamic traffic demand on a cycle-by-cycle basis. This insight has inspired us to investigate the potential benefits of combining MP control and signal coordination to develop a novel, network-level friendly, signal-coordinated strategy. Most importantly, feedback from Hennepin County and Minnesota Department of Transportation engineers repeatedly included a desire to add coordination into MP control. If MP control lacks coordination, then MP control could be a step backwards compared to current traffic signal timings.

Researcher may claim that, MP control is only proven to be a system stabilizer, i.e. it serves all demand whenever any other control could serve it, and it does not achieve any optimality in terms of the delay of traffic. Consequently, we are not surprised that network control with optimization formulations could outperform MP control in delay, such as Su et al. (2021)'s research. However, The downside of optimization formulations is that the problem is inherently stochastic due to turning proportions and entering vehicles, but the Markov decision process cannot be solved to optimality due to the curse of dimensionality as stated by Su et al. (2021). Therefore it is not clear whether their approach or others achieve the same level of stability as MP control. Our goal is to balance the two approaches: find a control that has the same stability properties as MP control but has better delay than prior MP control work by integrating standard signal timing practice.

The contributions of this paper are as follows: (1) We modify (Varaiya, 2013)'s max-pressure control policy to include signal coordination for the first time to develop Smoothing-MP. (2) We analytically prove the max-pressure control policy including signal coordination can also achieve maximum throughput at the network level without changing the stable region of the original MP control (Varaiya, 2013). (3) We implement our simulation using the Downtown Austin Network and a Grid Network with selected coordinated corridors.

The remainder of this paper is organized as follows: Section 2 summarizes the related research about signal coordination methods and MP control policies. Section 3 formulates the network model with signal coordination, vehicle queueing model, stable network definition, and stable region. These contents are prerequisites for proving maximum stability for the MP control, Smoothing-MP. Section 4 proposed the Smoothing-MP and stability analysis. Section 5 presents the simulation results and we conclude in Section 6.

#### 2. Literature review

In this section, we first review related papers focusing on traffic signal coordination. Then we review the existing literature on max-pressure (MP) signal control and back-pressure (BP) signal control.

#### 2.1. Traffic signal coordination

Traffic engineers have observed that by implementing appropriate signal timing at a series of signalized intersections, it is possible for vehicles to travel through the entire stretch without having to stop, as long as they maintain a suitable speed. This is now the concept of signal coordination (Feng, 2015). Some past research showed that the efficiency of urban traffic systems can be improved significantly through proper signal coordination strategies (Ma et al., 2016; Yao et al., 2019; Girault et al., 2016). For instance, Girault et al. (2016) provided a comprehensive analysis of signal coordination strategies on the macroscopic fundamental diagram of urban traffic. They leveraged seven signal coordination strategies under four kinds of demand patterns to figure out the impacts of signal coordination. The results showed that good signal coordination strategies have positive impacts on the macroscopic fundamental diagram. Ma et al. (2018a) claimed that signal coordination is one of the most economical ways to reduce urban traffic congestion.

In the field of signal coordination, traditional strategies are generally classified into two main categories: those aiming to maximize bandwidth along corridors, and those focusing on minimizing performance indices like the number of stops and vehicle delays. Historically, the MAXBAND method, introduced by Little et al. (1981), was a pioneering approach in the bandwidth maximization category. It was designed to optimize the green wave bandwidth along arterials using a branch and bound method. Despite its initial contributions, MAXBAND faced limitations, particularly in uniform bandwidth allocation and performance in extended arterials or network-level applications. This led to the development of enhanced methods, such as MULTIBAND by Gartner et al. (1991), which offered variable bandwidth progressions tailored to different traffic patterns, and adaptations like MaxBandLA and MaxBandGN by Zhang et al. (2016) for long arterials and grid networks. Further advancements include OD-NETBAND by Arsava et al. (2018) and PM-BAND by Ma et al. (2018b), addressing specific needs like major origin–destination flows and integrating transit vehicles within signal optimization frameworks. Conversely, in the category of minimizing performance indices, TRANSYT, developed by Dennis Robertson in the 1960s (Robertson, 1969), stands out. It optimizes cycle length, green splits, and offsets across network intersections. Notable improvements to this method include the time-dependent TRANSYT model by Wong et al. (2002) for dynamic traffic patterns, and the integration of TRANSYT with GIS systems for enhanced data handling, as proposed by de Oliveira and Ribeiro (2001).

Some researchers started to give more attention to future traffic environments and emergency technologies with signal coordination. Specifically, with the emergence of advanced sensors and mobile phone data, some research started focusing on developing data-driven methods to achieve signal coordination (Yao et al., 2019). For instance, Hu and Liu (2013) proposed a data-driven approach to optimize offsets for vehicle-actuated coordinated traffic signals, using the massive amount of signal status and vehicle actuation data collected from the field. The proposal was tested on a realistic scenario, a major arterial in Minnesota, USA. The result showed that the proposed method can reduce travel delays significantly. DiDi Chuxing also provided a huge set of trajectory data (Pian et al., 2020), which can provide more accurate traffic performance measures than traditional sensors. Due to the complexity of signal optimization and coordination problems, traffic signal researchers started looking at cloud computing. For instance, Zhang and Zhou (2018) proposed a coarse-grained parallel adaptive genetic algorithm (CPAGA) for the optimization of distributed coordination control, which considered the optimization of cycles, offsets, and green ratios on the cloud computing platform. The results demonstrated their proposed algorithm will not fall into a local optimum and finds a solution quickly. Learningbased methods are also becoming popular in solving transportation problems (Wei et al., 2021). Liu et al. (2021) proposed a multi-agent signal coordination framework based on reinforcement learning to achieve global optimal in the large-scale traffic network. Their proposed method is more scalable in practice. The future connected and autonomous vehicles (CAVs) environment is exciting for transportation participants (Fagnant and Kockelman, 2015). Signal control researchers also studied the opportunity brought by CAVs (Guo et al., 2019). Qi et al. (2020) invested in signalized intersection coordination design under mixed traffic flow conditions, which included human-driven vehicles and connected and autonomous vehicles. Das et al. (2022) proposed a priority-based traffic signal coordination system, which is able to consider multi-model traffic priority and vehicle actuation under the connected vehicle environment. The signal optimization model was formulated as a mixed-integer program and they tested the proposed signal control method in Anthem, Arizona, and in Portland, Oregon with satisfactory performance.

Furthermore, researchers also have a great interest in considering environmental impacts with signal coordination. Zhou et al. (2021) integrated emission reduction into signal coordination optimization problem. They formulated a bi-level multi-target optimization problem, which is able to achieve smooth traffic operation and minimize total emissions in the road network. Lv and Zhang (2012) aimed to investigate the impacts of signal coordination on traffic emissions, and the coordination quality is quantified by the platoon ratio, which is calculated by the ratio of flow rate during green to the average flow rate in the entire cycle.

However, most of these papers tried to model traffic signal coordination problems as mixed-integer programs, which are computationally difficult to solve at the network level. Although some papers try to provide a decentralized method to make signal coordination more scalable, they did not provide a rigorous mathematical proof of the maximum throughput of their signal control policy.

#### 2.2. Max-pressure signal control

Max-pressure (MP) signal control, also known as back-pressure (BP) signal control, is one type of decentralized signal control method. Initially, MP control was developed for scheduling methods in communication and power systems (Tassiulas and Ephremides, 1990). Later on, Varaiya (2013) brought the idea into signal control for the first time, and proved that the proposed MP signal control can stabilize the traffic network whenever possible. In Varaiya (2013)'s study, the traffic state was based on the link occupancy.

Practicality is important for checking whether a signal system can be put into use effectively. Varaiya (2013)'s original MP has a non-cyclical phase selection, which means it activates phases in arbitrary order to serve the movement with the highest pressure. However, the non-cyclical phase selection is not acceptable in practice since the phase order is confusing for drivers. To overcome these limitations, some research proposed cyclic-based MP signal controls (Le et al., 2015; Levin et al., 2020; Ma et al., 2020; Anderson et al., 2018). Le et al. (2015)'s cyclic-based MP signal control has a fixed cycle time and phases with varying phase durations. Anderson et al. (2018) also provided a cyclic-based MP controller which was inspired by the case of traffic signals usually updating green splits based on "cycle times" of 60–120 s, and simulated it of an arterial network. Later on, Ma et al. (2020) provided one kind of MP-based optimization method that combines fixed-phases sequences for oversaturated traffic conditions for the first time. Levin et al. (2020) provided a more flexible cyclic-based MP control with varying cycle durations in the form of a model predictive control with one cycle lookahead. Afterwards, Barman and Levin (2022) provided a novel semi-cyclic MP controller that addressed the limitations of non-cyclic MP controllers of more gridlock and longer waiting times, and the limitations of cyclic MP controllers such as higher loss time. The complexity of participants in urban transportation, including pedestrians, necessitates the consideration of traffic safety (Li et al., 2023; Xu, 2023). Consequently, researchers have begun to explore multimodal transportation systems. Xu et al. (2022a) modified MP control for public transit signal priority, and Xu et al. (2024a) incorporated pedestrian access.

However, budget limitations and the cost-benefit ratio make it impractical to install MP at all intersections. To solve this problem, Barman and Levin (2023) developed a method to find the best intersections to install the MP controllers, and provided stability analysis under limited deployment. Some research mentioned that it is more practical to estimate travel time information than vehicle queue length in reality. Therefore (Mercader et al., 2020) proposed a travel-time based MP controller and conducted experiments at an intersection in Jerusalem. Their results showed the applicability of travel-time-based MP and mentioned that the travel-time-based MP controller can still inherent capacity-aware properties.

The maximum stability proof is important since it establishes the maximum throughput property of MP control (Varaiya, 2013; Gregoire et al., 2014; Xiao et al., 2015b,a). However, since it is complex to provide a rigorous proof of stability, some MP research did not provide a stability proof. For instance, Sun and Yin (2018) constructed VISSIM simulations based on realistic scenarios at Newberry Road in Gainesville, FL. Their results showed that Varaiya (2013)'s non-cyclic MP control will have better performance than cyclic-based MP, and non-cyclic MP signal control performed better than the current coordinated actuated traffic signal controller. Mercader et al. (2020) provided a real-world experiment testing the proposed travel-time MP controller, but they did not provide the maximum stability proof. Chang et al. (2020) proposed a cyber-physical oriented traffic signal control that can improve the utilization of the MP control policy by preventing the frequent change of signal phases. Yu et al. (2021) leveraged the double queue model in pressure-based signal control and named it as a novel double pressure (DP) signal control to capture traffic dynamics. Experiments in two different networks showed that the proposed DP signal control can improve network travel time and queue stability. Dixit et al. (2020) leveraged crowdsourced delay data as the input for MP signal timing.

With the emergence of artificial intelligence technology, connected and autonomous vehicles can also be integrated into MP controllers. Liu and Gayah (2022) proposed a novel delay-based MP controller since the authors consider travel delay to be a more reasonable index than travel time or queue length. Rey and Levin (2019) also introduced the concept of the blue phase into the MP controller, which can coordinate autonomous vehicles at the network and achieve maximum throughput at the same time. With the emergency of artificial intelligence technology, many researchers tried to leverage reinforcement learning (RL) knowledge to MP control (Wei et al., 2019; Maipradit et al., 2021; Boukerche et al., 2021; Wang et al., 2022). Some research has begun to leverage MP control policies in vehicle dispatching to maximize throughput for shared autonomous vehicle operations in urban networks (Xu et al., 2021, 2024b; Robbennolt and Levin, 2023; Levin, 2022).

Some research combined route choice with signal control since user equilibrium route choice may reduce network throughput (Smith et al., 2019). Chen (2021) studied user equilibrium with the MP controller to figure out how the route choice behavior impacts the performance of the signal controller. Integrating route guidance or route control in MP controller can achieve dynamic traffic management. Taale et al. (2015) integrated signal control and route guidance based on the MP control and found that using travel time as a pressure variable performs better than using average density as a pressure variable. Zaidi et al. (2016) integrated fixed time and adaptive routing into a multi-commodity version of MP control policy and demonstrated that the proposed multi-commodity MP has significantly improved over the previous single-commodity MP. Smith et al. (2019) showed that user equilibrium route choice could cause the MP controller to fail to achieve maximum throughput.

In addition, the original MP signal control (Varaiya, 2013) is based on the point-queue model (Vickrey, 1969; Zhang et al., 2013), which is unrealistic. Therefore, researchers started focusing on MP controls that can consider the spatial distribution of traffic dynamics over the road. For example, Li and Jabari (2019) proposed a position-weighted back-pressure signal (PWBP) control policy based on a more accurate model of traffic flow. However, their proposed method is difficult to implement in practice since we cannot obtain accurate density information over every continuous space of a link. Therefore, Xu et al. (2022b) proposed an approximate position-weighted back-pressure (APWBP) traffic signal control policy, which employs kinematic wave theory to estimate traffic states based on the loop detectors installed in the upstream and downstream ends along the links. They proved that APWBP can

Table 1 Notation.	
М	Set of movements
$\mathcal{N}$	Set of nodes
$\mathcal{A}$	Set of links
$\Gamma_i^+$	Set of outgoing links
$\Gamma_j^+ \ \Gamma_j^-$	Set of incoming links
$x_{ii}(t)$	Number of vehicles of the movement from link $i$ to link $j$ at time step $t$
$r_{ij}(t)$	Proportion of vehicles entering $i$ that will next move to $j$ .
$w_{ii}(t)$	Weight of vehicle turning movement from link $i$ to link $j$ at time step $t$
$d_i(t)$	Vehicle demand at entry link i
$s_{ij}(t)$	Actuation of turning movement from link $i$ to link $j$ at time step $t$
$\xi_{ij}$	weight placed on coordination associated with turning movement $(i, j)$
$c_{ij}(t)$	signal coordination indicator associated with turning movement $(i, j)$ at time step $t$
$y_{ij}(t)$	Signal control vehicle flow from link $i$ to link $j$ at time step $t$
$Q_{ij}$	Capacity of turning movement for private vehicles from link i to link j
$f_i$	Average vehicle traffic volume of link i.
M	the number of total movements of vehicles.

still maximize the network vehicle throughput and stabilize vehicle queueing length whenever possible. Furthermore, the proposed APWBP controller can capture traffic density dynamics along the link and stabilize the network at the same level as the PWBP controller. Noaeen et al. (2021) also introduced a decentralized network-level traffic signal control named DESRA, which leverages a shockwave queue length estimation model while can capture the queueing spillback. However, there is no existing research that combines MP signal timing with signal coordination to smooth traffic in the urban network.

#### 3. Max pressure control with coordination

### 3.1. Math notations

See Table 1.

#### 3.2. Road network model

Consider an urban network  $G = (\mathcal{N}, \mathcal{A})$  with nodes  $\mathcal{N}$  and links  $\mathcal{A}$ . The link set  $\mathcal{A}$  is divided into three subsets: the entry link set  $\mathcal{A}_e$ , the internal link set  $\mathcal{A}_i$ , and the exit link set  $\mathcal{A}_o$ . The entry and exit links are not realistic links; they are used for loading and removing vehicles. Entry links represent the points where vehicles can enter the network, while exit links are the sink links where vehicles leave the network once they reach their destination nodes. The internal links  $\mathcal{A}_i$  connect the intersections located inside the vehicle network. All links are modeled are point queues. Let  $\mathcal{M}$  be the set of all turning movements in the network. We use  $\Gamma_i^+$  and  $\Gamma_j^+$  to represent the sets of outgoing links and incoming links of nodes (intersections), respectively. One turning movement is a combination of two links, such as (i,j) and (j,k). Let  $x_{ij}(t)$  be the number of vehicles on link i waiting to move to link j at time t. Let  $d_i(t)$  be the demand of vehicles entering the network on link  $i \in \mathcal{A}_e$  at time t, which are independent identically distributed random variables with an average value of  $d_i$ . Let  $d_i$  be the maximum value of demand. Turning proportion  $r_{jk}(t)$  is the proportion of vehicles entering link j that will next move to link k at time t, which are independent identically distributed random variables with mean  $\bar{r}_{jk}$ . Usually, the turning proportions can be obtained from historical travel data.  $Q_{ij}$  is the capacity of the turning movement from link i to link j.

### 3.3. Vehicle queueing model

We use the store-and-forward model of Varaiya (2013) to track the queue propagation in the network under discretized time. For internal links, the queue evolution can be represented by the following equations:

$$x_{ij}(t+1) = x_{ij}(t) - y_{ij}(t) + \sum_{h \in \mathcal{A}} y_{hi}(t) \times r_{ij}(t)$$
 (1)

where  $y_{ij}(t)$  is the signal controlled flow that start from link i then travels to link j at time step t. Vehicle flow conservation also applies to entry links with the following equation:

$$x_{ij}(t+1) = x_{ij}(t) - y_{ij}(t) + d_i(t) \times r_{ij}(t)$$
(2)

Therefore, the vehicle queue length state  $\mathbf{x}(t)$  can be formulated as a stochastic Markov chain since both vehicle demand  $\mathbf{d}(t)$  and turning proportion  $\mathbf{r}(t)$  are independent, identically distributed random variables.

The activation of vehicle turning movement (i, j) is denoted by  $s_{ij}(t) \in \{0, 1\}$ , which indicates a red light or green light. The value of  $y_{ij}(t)$  is determined by the following equation:

$$y_{ij}(t) = \min \left\{ Q_{ij} s_{ij}(t), x_{ij}(t) \right\}$$
 (3)

where  $Q_{ij}$  is the capacity of the turning movement from link i to link j. Specifically,  $Q_{ij} = \min(Q_i, Q_j)$ , is the maximum flow of vehicle movement (i, j). Note that capacity is the maximum road throughput, which we assume to be constant for each link.

#### 3.4. Feasible signal control including signal coordination

The activation of turning movement (i, j) for vehicles is denoted by  $s_{ij}(t) \in 0$ , 1.  $s_{ij}(t) = 1$  indicates that movement (i, j) has a green light, while  $s_{ij}(t) = 0$  signifies a red light for movement (i, j). We define  $S_n(t)$  as the intersection matrix for intersection n, which encompasses the vehicle movements. The intersection control sequence  $S_n$  is defined as  $S_n(t)$ , for all  $t \in T$ . Let S be the set containing all feasible network control matrices for all intersections, and let  $S_n$  be the set of all feasible intersection matrices for intersection n. We denote the convex hull of all feasible signal control matrices as Conv(S).

For any given intersection control sequence, the long-term average time used for serving vehicle movement (i, j) can be calculated using Eq. (4). Let  $\bar{s}$  and s(t) be the vectors of  $\bar{s}_{ij}$  and  $s_{ij}(t)$ , respectively:

$$\bar{s}_{ij} = \lim_{T \to \infty} \frac{1}{T} \sum_{t=1}^{T} s_{ij}(t) \tag{4}$$

The convex hull of all feasible signal control matrices S is given by the following equation:

$$Conv(S) = \left\{ \sum_{s \in S} \lambda_s S \middle| \lambda_s S \le 0, \sum_{s \in S} \lambda_s = 1 \right\}$$
 (5)

Conv(S), is the set of average controls calculated by Eq. (4). After that, we can give Proposition 1 to relate s(t) to  $\bar{s}$ .

**Proposition 1.** If  $s(t) \in S$  then there exists a  $\bar{s} \in Conv(S)$  such that

$$\bar{\mathbf{s}} = \lim_{T \to \infty} \frac{1}{T} \sum_{t=1}^{T} \mathbf{s}(t) \tag{6}$$

**Proof.** First, we prove that  $\bar{s}$  is in Conv(S). Let us define  $\lambda_s$  is the proportion of time steps with s = s(t). Then we can define the indicator function as

$$\mathbb{I}(\mathbf{s}(t) = \mathbf{s}) \begin{cases} 1 & \text{if } \mathbf{s}(t) = \mathbf{s} \\ 0 & \text{if } \mathbf{s}(t) \neq \mathbf{s} \end{cases}$$
 (7)

Then we have

$$\bar{\mathbf{s}} = \sum_{s \in S} \lambda_s \mathbf{s} \tag{8}$$

$$= \lim_{T \to \infty} \frac{1}{T} \sum_{t=1}^{T} \sum_{\mathbf{s} \in S} T \lambda_{\mathbf{s}} \mathbf{s}$$
 (9)

$$= \lim_{T \to \infty} \frac{1}{T} \sum_{t=1}^{T} \sum_{\mathbf{s}} \mathbb{I}(\mathbf{s}(t) = \mathbf{s})\mathbf{s}$$
 (10)

$$= \lim_{T \to \infty} \frac{1}{T} \sum_{t=1}^{T} \mathbf{s}(t) \quad \Box$$
 (11)

# 3.5. Max-pressure control policy that includes signal coordination

To incorporate signal coordination into the max-pressure control, we define  $c_{ij}(t)$  as the coordination indicator associated with movement (i,j) at time t. Define C to be the set of coordinated corridors. Each corridor  $C \in C$  is a subset of links (i.e.,  $C \subseteq A$ ) that are intended to be coordinated. Specifically,  $c_{jk}(t+1) = s_{ij}(t)$  for  $(i,j,k) \in C$  for some corridor C, with  $c_{ij}(t) \in \{0,1\}$ . Thus, if (i,j) has a green light at time step t, then (j,k) has a coordination indicator for a green light at time step t + 1. Overall, we can obtain a feasible signal control  $s_{ij}(t)$  that includes signal coordination.

Now we define the MP control. This study modifies the original MP control policy of Varaiya (2013) to create the max-pressure signal control policy that considering signal coordination (Smoothing-MP). The weight calculation is the same as previous papers (Varaiya, 2013; Levin et al., 2020; Xu et al., 2022a):

$$w_{ij}(t) = x_{ij}(t) - \sum_{k \in \Gamma_j^+} r_{jk}(t) x_{jk}(t)$$
(12)

After we calculate the weight for each movement, a mixed-integer linear program is used to calculate the intersection control. The modified MP control policy considering signal coordination tries to maximize the total pressure of vehicles.  $s_{ij}^{\star}(t)$  denotes the max-pressure signal control in the transportation network when considering signal coordination, which is

$$s_{ij}^{\star}(t) = \underset{s \in \mathcal{S}}{\arg \max} \left[ \sum_{(i,j) \in \mathcal{M}} s_{ij}(t) Q_{ij} w_{ij}(t) + \xi_{ij} c_{ij}(t) \right]$$
(13)

Note that  $\xi_{ij}$  is the weight placed on coordination, where  $\xi_{ij} \geq 0$ . Without such a bound, assigning an excessively large value to  $\xi_{ij}$  could result in perpetual prioritization of one direction, effectively preventing vehicles from the conflicting direction from proceeding. The upper bound should be judiciously determined in relation to the traffic movement capacity, represented by  $Q_{ij}$ . For instance, in a situation where the upstream is operating at full capacity and the downstream is unoccupied, the upper limit of  $\xi_{ij}$  should correspond to  $Q_{ij}^2$  when  $x_{ij}(t)$ , the traffic density at time t, meets movement capacity.

Furthermore, the traditional concept of signal coordination focuses on synchronizing traffic lights along arterial corridors to provide continuous green lights, thereby reducing the average number of stops and delays. In our research, the function  $c_{ij}(t)$  is formulated to achieve a similar 'coordinate' target. Specifically, we propose  $c_{jk}(t+1) = s_{ij}(t)$ , implying that for every link i, j, k in a coordinated corridor, the downstream traffic light will be influenced by the previous time step and the upstream traffic light. This mechanism aims to establish a form of 'priority' to minimize stops and delays.

The extent of coordination depends on the flow from i to j to k, as well as the value of  $\xi_{ij}$ . This setup closely aligns with the principle of signal coordination, as downstream traffic lights are coordinated or affected by upstream traffic to coordinate flow along a chosen corridor. Therefore, while our work indeed encompasses aspects of network-wide traffic control, the methodology and objectives also resonate with the concept of signal coordination, particularly in the context of managing traffic flow along specific corridors.

To compare the modified max-pressure signal control policy, Smoothing-MP, with both (Varaiya, 2013)'s original max pressure control and the average signal control, we propose the following Lemma:

**Lemma 1.** If the modified max-pressure signal control policy, Smoothing-MP, is used and  $\bar{\mathbf{d}} \in \mathcal{D}^0$ , then we have the following inequality with average signal control  $\bar{s}_{i,i}$  satisfying Eq. (22):

$$\mathbb{E}\left[\sum_{(i,j)\in\mathcal{M}^2} s_{ij}^{\star}(t)Q_{ij}w_{ij}(t) + \xi_{ij}c_{ij}(t)\bigg|\mathbf{x}(t)\right] \ge \mathbb{E}\left[\sum_{(i,j)\in\mathcal{M}^2} \bar{s}_{ij}Q_{ij}w_{ij}(t)\bigg|\mathbf{x}(t)\right]$$
(14)

**Proof.** First, we have the following inequality based on definition of MP control. For all  $s_{ij}(t) \in S$ :

$$\sum_{(i,j)\in\mathcal{M}^2} s_{ij}^{\star}(t)Q_{ij}w_{ij}(t) \ge \sum_{(i,j)\in\mathcal{M}^2} s_{ij}(t)Q_{ij}w_{ij}(t) \tag{15}$$

After we include signal coordination, we have the following inequality, since both  $\xi_{ij}$  and  $c_{ij}(t)$  are non-negative:

$$\sum_{(i,j)\in\mathcal{M}^2} s_{ij}^{\star}(t)Q_{ij}w_{ij}(t) + \xi_{ij}c_{ij}(t) \ge \sum_{(i,j)\in\mathcal{M}^2} s_{ij}^{\star}(t)Q_{ij}w_{ij}(t)$$
(16)

Then we have

$$\sum_{(i,j)\in\mathcal{M}^2} s_{ij}^{\star}(t)Q_{ij}w_{ij}(t) + \xi_{ij}c_{ij}(t) \ge \sum_{(i,j)\in\mathcal{M}^2} s_{ij}^{\star}(t)Q_{ij}w_{ij}(t) \ge \sum_{(i,j)\in\mathcal{M}^2} s_{ij}(t)Q_{ij}w_{ij}(t)$$
(17)

Then calculating the expected value of Eq. (15) when given the vehicle queue length x(t), and taking the expected value. Because there exists an  $s_{ij}(t)$  with  $\mathbb{E}[s_{ij}(t)] = \bar{s}_{ij}$  by Proposition 1, we have following inequality:

$$\mathbb{E}\left[\sum_{(i,j)\in\mathcal{M}^2} s_{ij}^{\star}(t)Q_{ij}w_{ij}(t) + \xi_{ij}c_{ij}(t)\bigg|\mathbf{x}(t)\right] \ge \mathbb{E}\left[\sum_{(i,j)\in\mathcal{M}^2} \bar{s}_{ij}Q_{ij}w_{ij}(t)\bigg|\mathbf{x}(t)\right] \quad \Box$$
(18)

# 4. Stability analysis

One major advantage of MP control is its mathematically proven network stability. Therefore, it is crucial to provide the stability analysis for the modified MP control, Smoothing-MP.

#### 4.1. Stable network

We can mathematically define stability as follows:

**Definition 1.** The network is strongly stable if the number of vehicles in the network is bounded in expectation, i.e. there exists a  $\kappa < \infty$  such that

$$\lim_{T \to \infty} \sup \left\{ \frac{1}{T} \sum_{t=1}^{T} \sum_{(i,j) \in \mathcal{A}^2} \mathbb{E}\{x_{ij}(t)\} \right\} \le \kappa \tag{19}$$

Stability means the ability/capacity of network-level signal controls to serve all demand in the transportation network. If a network is stable, the total expected queue length will remain bounded in the long run. It is easy for us to find a large demand rate such that no traffic control policy can serve it, such as a very large demand that exceeds the turning movement capacity  $Q_{ij}$ . Therefore, to prove the maximum-stability property of a signal control policy, we need to define the network stable region.

#### 4.2. Stable region

The primary objective of MP control is to stabilize any vehicle demand that could be stabilized by any other signal control. To prove the maximum stability property, we must analytically define the set of vehicle demands that can be stabilized. Since the demand is stochastic, the stable region is defined in terms of the average demand rates  $\bar{\mathbf{d}}$ .

Let **f** be the average volume of vehicles on link *i*. For entry links, we have the following relationship between the average volume of vehicles and demand:

$$f_i = \bar{d}_i$$
 (20)

For internal links of vehicles,  $f_i$  can be determined by conservation of flow, which means the total flow on the downstream link is determined from all flow on the upstream link moving to the downstream link:

$$f_j = \sum_{i \in A} f_i \bar{r}_{ij} \tag{21}$$

By Proposition 1 of Varaiya (2013), for every demand rate  $\bar{d}$  and turning proportions  $\bar{r}$ , there exists a unique average flow vector f. In this study, the network can be stabilized if the average vehicle flow can still be served by some traffic signals, considering the signal coordination. That is, there must exist an average signal activation  $\bar{s} \in S$  that can serve the demand. It is crucial to mention that the stable region in this study is the same as the stable region in Varaiya (2013), since we aim to prove that our proposed signal control policy can still achieve maximum throughput.

$$f_i \bar{r}_{ij} \le \bar{s}_{ij} Q_{ij} \tag{22}$$

where  $\bar{s}_{ij}$  can be obtained from Eq. (4).

Let  $\vec{D}$  be the set of all feasible demand vectors of vehicles  $\vec{\bf d}$ . Let  ${\cal D}^0$  be the interior of  ${\cal D}$ , where constraints (22) hold with strict inequality. Then there exists an  $\epsilon > 0$  such that

$$f_i \bar{r}_{ii} - \bar{s}_{ii} Q_{ii} \le -\epsilon$$
 (23)

If the network is unstable, at least one link has a flow greater than the traffic signal control policy can serve. Or we can say, If  $\bar{\mathbf{d}} \notin \mathcal{D}$ , then it is impossible to find a stabilizing control (Varaiya, 2013).

#### 4.3. Stability analysis for Smoothing-MP

**Lemma 2.** If Smoothing-MP is used and  $\bar{\mathbf{d}} \in \mathcal{D}^0$ , there exists a Lyapunov function  $v(t) \geq 0$  and constants  $\kappa > 0$ ,  $\epsilon > 0$  such that

$$\mathbb{E}\left[v(t+1) - v(t)|\mathbf{x}(t)\right] \le \kappa - \eta|\mathbf{x}(t)| \tag{24}$$

**Proof.** To calculate the queue length at time t + 1, we apply the vehicle queueing models shown in Eq. (1)–(3). Then, let  $\delta_{ij}(t)$  be the difference of the queueing length of vehicles between time steps t and time steps t + 1.

$$\delta_{ij}(t) = x_{ij}(t+1) - x_{ij}(t) \tag{25}$$

$$= -y_{ij}(t) + \sum_{h \in A} y_{hi}(t) \times r_{ij}(t)$$
 (26)

$$= -\min\left\{Q_{ij}s_{ij}(t), x_{ij}(t)\right\} + \sum_{h \in \mathcal{A}_i^-} \min\left\{Q_{hi}s_{ij}(t), x_{hi}(t)\right\} \times r_{ij}(t) \quad \forall i \in \mathcal{A}_i, j \in \Gamma_i^+$$

$$(27)$$

For entry links, we have

$$\delta_{ij}(t) = x_{ij}(t+1) - x_{ij}(t) = -y_{ij}(t) + d_i(t) \times r_{ij}(t) = -\min\left\{Q_{ij}s_{ij}(t), x_{ij}(t)\right\} + d_i(t) \times r_{ij}(t) \quad \forall i \in \mathcal{A}_e, j \in \Gamma_i^+$$
(28)

Let  $\mathbf{x}(t)$  be the matrix including all queue length of private vehicles. Hence we consider the Lyapunov function v(t):

$$v(t) = \left| \mathbf{x}(t) \right|^2 = \sum_{(i,i) \in A^2} (x_{ij}(t))^2$$
 (29)

Then we expand the difference  $v_1(t+1) - v_1(t)$ :

$$v(t+1) - v(t) = \left| \mathbf{x}(t+1) \right|^2 - \left| \mathbf{x}(t) \right|^2 = \left| \mathbf{x}(t) + \delta(t) \right|^2 - \left| \mathbf{x}(t) \right|^2 = 2\mathbf{x}(t)^{\mathrm{T}} \delta(t) + \left| \delta(t) \right|^2$$
(30)

The first term of Eq. (30) can be rewritten as:

$$\begin{split} 2\mathbf{x}(t)^{\mathrm{T}}\boldsymbol{\delta}(t) &= -2x_{ij}(t)\sum_{i\in\mathcal{A}}\sum_{j\in\Gamma_{i}^{+}}\min\left\{Q_{ij}s_{ij}(t),x_{ij}(t)\right\} \\ &+ 2\sum_{h\in\Gamma_{i}^{-}}\sum_{i\in\mathcal{A}}\sum_{j\in\Gamma^{+}}x_{ij}(t)\min\left\{Q_{hi}s_{hi}(t),x_{hi}(t)\right\}r_{ij}(t) \end{split}$$

$$+ 2 \sum_{i \in \mathcal{A}_e} \sum_{j \in \Gamma^+} (-\min \left\{ Q_{ij} s_{ij}(t), x_{ij}(t) \right\} + d_i(t) \times r_{ij}(t))$$
(31)

$$=2\sum_{i\in\mathcal{A}_{i}\cup\mathcal{A}_{e}}\sum_{j\in\Gamma_{i}^{+}}\min\left\{Q_{ij}s_{ij}(t),x_{ij}(t)\right\}\left(-x_{ij}(t)+\sum_{k\in\Gamma_{i}^{+}}r_{jk}(t)x_{jk}(t)\right)$$

$$+2\sum_{i\in\mathcal{A}_{e}}\sum_{j\in\Gamma_{i}^{+}}d_{i}(t)\times r_{ij}(t)\times x_{ij}(t)$$
(32)

We replace the turning proportion  $r_{ij}(t)$  with average value  $\bar{r}_{ij}$ , since  $\mathbb{E}[r_{ij}(t)] = \sum_{i,j \in \mathcal{A}} \bar{r}_{ij}$ . Therefore we have the following equation:

$$\mathbb{E}[\mathbf{x}(t)^{\mathrm{T}}\boldsymbol{\delta}(t)|\mathbf{x}(t)] = \sum_{i \in \mathcal{A}_{i} \cup \mathcal{A}_{e}} \sum_{j \in \Gamma_{i}^{+}} \mathbb{E}\left[\min\left\{Q_{ij}s_{ij}(t), x_{ij}(t)\right\} \times \left(-x_{ij}(t)\right) \middle| \mathbf{x}(t)\right]$$

$$+ \sum_{i \in \mathcal{A}_{i} \cup \mathcal{A}_{e}} \sum_{j \in \Gamma_{i}^{+}} \mathbb{E}\left[\min\left\{Q_{ij}s_{ij}(t), x_{ij}(t)\right\} \middle| \mathbf{x}(t)\right] \times \left(\sum_{k \in \Gamma_{i}^{+}} \bar{r}_{jk}x_{jk}(t)\right)$$

$$+ \sum_{i \in \mathcal{A}_{i}} \sum_{j \in \Gamma_{i}^{+}} \mathbb{E}\left[d_{i}(t)\bar{r}_{ij}x_{ij}(t) \middle| \mathbf{x}(t)\right]$$

$$(33)$$

Then we obtain

$$\mathbb{E}[\mathbf{x}(t)^{\mathrm{T}}\boldsymbol{\delta}(t)|\mathbf{x}(t)] = \sum_{i \in \mathcal{A}_{i} \cup \mathcal{A}_{e}} \mathbb{E}\left[\min\left\{Q_{ij}s_{ij}(t), x_{ij}(t)\right\} \left|\mathbf{x}(t)\right] \times \left(-x_{ij}(t) + \sum_{k \in \Gamma_{i}^{+}} \bar{r}_{jk}x_{jk}(t)\right) + \sum_{i \in \mathcal{A}_{i}} \bar{d}_{i}\bar{r}_{ij}x_{ij}(t) \right]$$

$$(34)$$

Based on Eqs. (4)-(34) and the definition of pressure term (12), we obtain

$$\mathbb{E}[\mathbf{x}(t)^{\mathrm{T}}\boldsymbol{\delta}(t)|\mathbf{x}(t)] = \sum_{i \in \mathcal{A}_{i} \cup \mathcal{A}_{e}} \mathbb{E}\left[\min\left\{Q_{ij}s_{ij}(t), x_{ij}(t)\right\} \left|\mathbf{x}(t)\right] \times (-w_{ij}(t)) + \sum_{i \in \mathcal{A}_{e}} \bar{d}_{i}\bar{r}_{ij}x_{ij}(t)\right]$$
(35)

The last term of Eq. (35) can be rewritten as follows based on Eqs. (20), (21), and (12):

$$\sum_{i \in A_{-}} \bar{d}_{i} \bar{r}_{ij} x_{ij}(t) = \sum_{i \in A_{-}} f_{ij} x_{ij}(t)$$
(36)

$$= \sum_{i \in A_{-1} \cup A_{-}} f_i \bar{r}_{ij} x_{ij}(t) - \sum_{i \in A_{-}} f_j \bar{r}_{jk} x_{jk}(t)$$
(37)

$$= \sum_{i \in \mathcal{A}_e \cup \mathcal{A}_e} f_i \bar{r}_{ij} x_{ij}(t) - \sum_{j \in \Gamma_i^+} \left[ f_i \bar{r}_{ij} \right] \sum_{k \in \Gamma_i^+} \bar{r}_{jk} x_{jk}(t) \tag{38}$$

$$= \sum_{i \in \mathcal{A}_i \cup \mathcal{A}_n} f_i \bar{r}_{ij} \left( w_{ij}(t) \right) \tag{39}$$

Combining Eqs. (35) and (39) yields

$$\mathbb{E}[\mathbf{x}(t)^{\mathrm{T}}\boldsymbol{\delta}(t)|\mathbf{x}(t)] = \sum_{i \in \mathcal{A}_{i} \cup \mathcal{A}_{e}} \left( f_{i}\bar{r}_{ij} - \mathbb{E}\left[\min\left\{Q_{ij}s_{ij}(t), x_{ij}(t)\right\} \middle| \mathbf{x}(t)\right] \right) w_{ij}(t)$$

$$= \sum_{i \in \mathcal{A}_{i} \cup \mathcal{A}_{e}} \left( f_{i}\bar{r}_{ij} - Q_{ij}s_{ij}^{\star}(t) \right) w_{ij}(t)$$

$$= \sum_{i \in \mathcal{A}_{i} \cup \mathcal{A}_{e}} \left( f_{i}\bar{r}_{ij} - Q_{ij}s_{ij}^{\star}(t) \right) w_{ij}(t)$$

$$+ \sum_{i \in \mathcal{A}_i \cup \mathcal{A}_e} \left( Q_{ij} s_{ij}^{\star}(t) - \mathbb{E} \left[ \min \left\{ Q_{ij} s_{ij}(t), x_{ij}(t) \right\} \middle| \mathbf{x}(t) \right] \right) w_{ij}(t)$$

$$(41)$$

For the second term of Eq. (41), if  $x_{ij}(t) \ge Q_{ij}$ , then we have  $\mathbb{E}\left[\min\left\{Q_{ij}s_{ij}(t), x_{ij}(t)\right\} \middle| \mathbf{x}(t)\right]$ =  $Q_{ij}s_{ij}^{\star}(t)$ . Therefore, the second term of Eq. (41) equals zero. If  $x_{ij}(t) < Q_{ij}$  and  $s_{ij}(t) \ne 0$ , then we have  $\mathbb{E}\left[\min\left\{Q_{ij}s_{ij}(t),x_{ij}(t)\right\}\bigg|\mathbf{x}(t)\right]=\mathbb{E}\left[x_{ij}(t)\bigg|\mathbf{x}(t)\right]$ . Therefore, we obtain the following inequality

$$\left(Q_{ij}s_{ij}^{\star}(t) - \mathbb{E}\left[x_{ij}(t)\middle|\mathbf{x}(t)\right]\right)w_{ij}(t) \le Q_{ij}x_{ij}(t) \le (Q_{ij})^{2}$$

$$\tag{42}$$

Hence, the second term of Eq. (41) equals zero or is bounded by  $\sum_{i \in A_i \cup A_e} (Q_{ij})^2$ . The modified MP control  $s_{ij}^{\star}(t)$  is chosen from the feasible signal control set S, and  $s_{ij}^{\star}(t)$  seeks to maximize the objective (13). According to Lemma 1, we following inequality:

$$\mathbb{E}\left[\sum_{i \in \mathcal{A}_i \cup \mathcal{A}_e} \left[ f_i \bar{r}_{ij} - s_{ij}^{\star}(t) Q_{ij} \right] w_{ij}(t) - \xi_{ij} c_{ij}(t) \middle| w_{ij}(t) \right] \le \mathbb{E}\left[\sum_{i \in \mathcal{A}_i \cup \mathcal{A}_e} \left[ f_i \bar{r}_{ij} - s_{ij}^{\star}(t) Q_{ij} \right] w_{ij}(t) \middle| w_{ij}(t) \right]$$

$$\tag{43}$$

T. Xu et al.

and

$$\mathbb{E}\left[\sum_{i \in \mathcal{A}_i \cup \mathcal{A}_e} \left[ f_i \bar{r}_{ij} - s_{ij}^{\star}(t) Q_{ij} \right] w_{ij}(t) \middle| w_{ij}(t) \right] \le \mathbb{E}\left[\sum_{i \in \mathcal{A}_i \cup \mathcal{A}_e} \left[ f_i \bar{r}_{ij} - \bar{s}_{ij} Q_{ij} \right] w_{ij}(t) \middle| w_{ij}(t) \right]$$

$$(44)$$

Therefore, for some feasible signal controls  $s_{ij}(t)$  satisfying the stable region, we obtain  $\bar{s}_{ij}$  based on Eq. (4). We have the following relationship for the first term of Eq. (41) based on Eq. (23) when  $\bar{\mathbf{d}} \in \mathcal{D}^0$ :

$$\sum_{i \in A \cup A} \left[ f_i \bar{r}_{ij} - \bar{s}_{ij} Q_{ij} \right] w_{ij}(t) \le -\epsilon \sum_{ij} \max \left\{ w_{ij}, 0 \right\} \le -\epsilon |w_{ij}| \tag{45}$$

We know that the pressure  $\mathbf{w}(t)$  is a linear function of the queue length of vehicles. So we can find  $\beta > 0$  to satisfy  $\sum_{(i,j) \in \mathcal{M}^2} w_{ij} \ge \beta |\mathbf{x}|$ . Then we have

$$-\epsilon |w_{ij}| \le -\epsilon \beta |\mathbf{x}| \le \sum_{i \in A: \cup A.} (Q_{ij})^2 - \epsilon \beta |\mathbf{x}| \tag{46}$$

Eq. (24) satisfies the following relationship based on Eqs. (44) and (45). For  $\delta_{ii}(t)$ 

$$\left|\delta_{ij}(t)\right| = \left|-\min\left\{Q_{ij}s_{ij}(t), x_{ij}(t)\right\} + \sum_{h \in \mathcal{A}_i^-} \min\left\{Q_{hi}s_{ij}(t), x_{hi}(t)\right\} \times r_{ij}(t)\right| \quad \forall i \in \mathcal{A}_i, j \in \Gamma_i^+$$

$$(47)$$

$$\leq \max \left\{ Q_{ij}, \sum_{h \in \mathcal{A}_i^-} Q_{ij} \right\} \tag{48}$$

Then we have

$$\left|\delta_{ij}(t)\right| = \left|-\min\left\{Q_{ij}s_{ij}(t), x_{ij}(t)\right\} + d_i(t) \times r_{ij}\right| \le \max\left\{Q_{ij}, \hat{d}_{ij}\right\} \quad \forall i \in \mathcal{A}_{e}, j \in \Gamma_i^+$$

$$\tag{49}$$

Define w follows

$$\psi = \max \left\{ Q_{ij}, \sum_{h \in \mathcal{A}_i^-} Q_{ij}, \hat{d}_{ij} \right\}$$
(50)

Because the number of total movements of vehicles is M, we have the following inequality:

$$\left|\delta_{ij}(t)\right|^2 \le M \times \psi^2 \tag{51}$$

Since  $\delta_{ij}(t)$  is upper-bounded by  $\max\left\{Q_{ij}, \sum_{h \in \mathcal{A}_i^-} Q_{ij}\right\}$ , we can use Eq. (46), along with Eqs. (48)–(51), to derive the following:

$$\left|\mathbf{x}(t+1)\right|^{2} - \left|\mathbf{x}(t)\right|^{2} = 2\mathbf{x}(t)^{\mathrm{T}}\boldsymbol{\delta} + \left|\boldsymbol{\delta}\right|^{2}$$

$$\leq 2\left(\sum_{i \in A: \cup A_{-}} (Q_{ij})^{2} - \epsilon \boldsymbol{\beta}|\mathbf{x}(t)|\right) + M\psi^{2}$$
(52)

$$=\kappa - \eta |\mathbf{x}(t)| \tag{53}$$

where  $\kappa = 2 \sum_{i \in A_i \cup A_o} (Q_{ij})^2 + M \psi^2$  and  $\epsilon \beta = \eta$ .  $\square$ 

**Proposition 2.** *Smoothing-MP* is stabilizing when  $\bar{\mathbf{d}} \in \mathcal{D}^0$ .

**Proof.** Inequality (24) holds from Lemma 2. Taking expectations, summing over t = 1, ..., T, and transferring the position of terms gives the following inequality:

$$\mathbb{E}\left[\left|v(T+1)-v(1)\right|\mathbf{x}(t)\right] \le \kappa T - \epsilon \sum_{t=1}^{T} |\mathbf{x}(t)| \tag{54}$$

Then we have

$$\epsilon \frac{1}{T} \sum_{t=1}^{T} \mathbb{E}\left[|\mathbf{x}(t)|\right] \le \kappa - \frac{1}{T} \mathbb{E}\left[\nu(T+1)\right] + \frac{1}{T} \mathbb{E}\left[\nu(1)\right] \le \kappa + \frac{1}{T} \mathbb{E}\left[\nu(1)\right]$$
(55)

which implies that Definition 1 is satisfied.

Moreover, we need to mention that stability is not impacted by the initial condition. Let us move  $\epsilon$  in to the right hand side and take the limit as T goes to infinity. Then the  $\frac{1}{T}\mathbb{E}\left[\nu(1)\right]$  term approaches zero, which yields the following inequality which implies Definition 1 is satisfied:

$$\lim_{T \to \infty} \frac{1}{T} \sum_{t=1}^{T} \mathbb{E}\left[|\mathbf{x}(t)|\right] \le \frac{\kappa}{\epsilon} \tag{56}$$

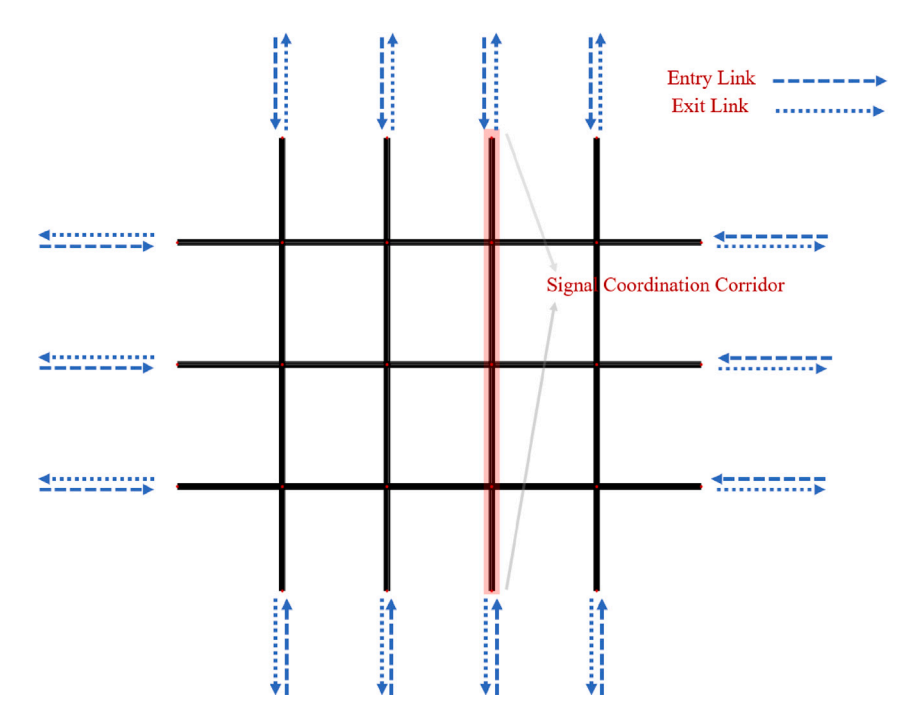


Fig. 1. Grid network with signal coordination corridor.

Since  $\bar{\mathbf{d}} \in \mathcal{D}^0$  and Definition 1 is satisfied, the network achieves maximum stability under the use of Smoothing-MP.

# 5. Multi-scenario simulation and numerical results

To evaluate the performance of the proposed Smoothing-MP control, we conducted simulations on two distinct networks: the Downtown Austin Network and a Grid Network. These test networks were chosen to ensure a robust and comprehensive assessment of the new method. The simulations were implemented using the microscopic traffic simulation tool, SUMO, interfaced with Python (Lopez et al., 2018). The locations of signal coordination corridors within the Downtown Austin Network and a Grid Network (GridNet) are illustrated in Figs. 1 and 2, respectively. The Downtown Austin Network consists of 546 nodes and 1247 links, and the network profile could be found through the authors' previous studies (Levin et al., 2020). This Grid Network consists of 12 nodes and 72 links. The empirical results, presented subsequently, offer a comparative evaluation between the proposed Smoothing-MP and the established MP control (Varaiya, 2013). It is worth noting that, apart from the controllers on the coordination corridors in both networks, all other signal controls adhere to the original MP control strategy.

#### 5.1. Stability comparison

This section focuses on verifying the stability of the network as per Definition 1. To this end, we conduct simulations to observe the total number of vehicles within the network and monitor whether it increases over time under various vehicle demand level settings.

Fig. 3 presents the average number of waiting vehicles within the Grid Network (GridNet). It reveals a striking consistency in the average number of waiting vehicles across different vehicle demand and coordination weight ( $\xi$  value) settings. The maximum stable region, identified across coordination weight settings (2000, 10000, 20000), lies within the range of 2400 to 2560 vehicles per hour, a value identical to that of the Original MP control. Similar observations can be made from the Austin Network results displayed in Fig. 4. Here, too, the average number of waiting vehicles remains approximately the same under varying vehicle demand and coordination weight ( $\xi$  value) settings. The maximum stable region for the different coordination weight settings (2000, 10000, 20000) is around 13530 vehicles per hour, aligning with the Original MP control. These findings lead us to conclude that the Smoothing-MP exhibits a stable region analogous to that of the Original MP control, corroborating the definition of the stable region discussed in Section 4.2.

# 5.2. Average speed

The goal of signal coordination is to improve the average speed along corridors. In the context of the Grid Network we use Fig. 5(a) demonstrates that the average speed along the corridor under the Original MP control surpasses that under the Smoothing-MP control for vehicle demand levels ranging from 800 to 3840 vehicles per hour. Conversely, Fig. 5(b) illustrates that the average



Fig. 2. Austin network with signal coordination corridor.

speed along the corridor's conflict direction is lower under the Original MP control than under the Smoothing-MP control within the same vehicle demand range.

For the Austin Network, similar patterns can be discerned, as depicted in Figs. 6(a) and 6(b). The former reveals that the average speed along the corridor under the Original MP control exceeds that under the Smoothing-MP control for vehicle demand ranging from 11070 to 15990 vehicles per hour. Meanwhile, the latter indicates that the average speed along the corridor conflict direction is reduced under the Original MP control compared to the Smoothing-MP control within the same vehicle demand range.

Both Figs. 5 and 6 consolidate the observation that vehicle travel speed along corridors can be increased under the Smoothing-MP controller. However, this augmentation comes at the expense of reduced average speed along corresponding conflict directions.

The influence of signal coordination weight value on the average speed dynamics along corridors and their conflict directions is another significant aspect to examine. Fig. 7(a) within the context of the Grid Network indicates that, given various vehicle demands, the average speed tends to increase in correlation with the signal coordination weight value along the corridor directions. In contrast, Fig. 7(b) shows that the average speed decreases as the signal coordination weight value increases along the corridor conflict directions.

Analogous patterns are observed for the Austin Network, as depicted in Figs. 8(a) and 8(b). As such, we can infer that higher signal coordination weight values are associated with increased average speeds along corridor directions, while a contrary pattern is evident along the corridor conflict directions. Please note that, Figs. 8(a) and 8(b) illustrate a comparison of the average speed metric for road links along the coordinated corridor (from North to South and South to North) and their adjacent conflicting road links (corridor conflict directions from East to West and West to East). This metric is not intended to indicate stability but rather to assess the operational efficiency of the coordinated corridor relative to its intersecting routes. It is important to distinguish that stability—reflected in our study as the average number of queuing vehicles—is a network-level metric used to ascertain the overall stability of the traffic network, which are shown in Figs. 3 and 4.

In addition, we present a time-series plot of the average vehicle speed along the corridor for each simulation time in Fig. 9. Analysis of these findings suggests that the implementation of the Smoothing-MP algorithm along signal coordination corridors results in more stable and higher average vehicle speed dynamics, which approximate free flow speed. In contrast, the Original MP control produces significantly more fluctuation in the average vehicle speed along the corridor, indicating less stability than when the Smoothing-MP control is employed.

#### 5.3. Average delay

Average delay is a widely accepted metric in traffic signal studies (Liu and Gayah, 2022; Wang et al., 2022; Xu et al., 2024a, 2022b). Consequently, we present the average delay values along the corridors and their corresponding conflict directions. For the Grid Network's corridor direction, the average delay tends to increase with vehicle demand. Moreover, the average delay under the

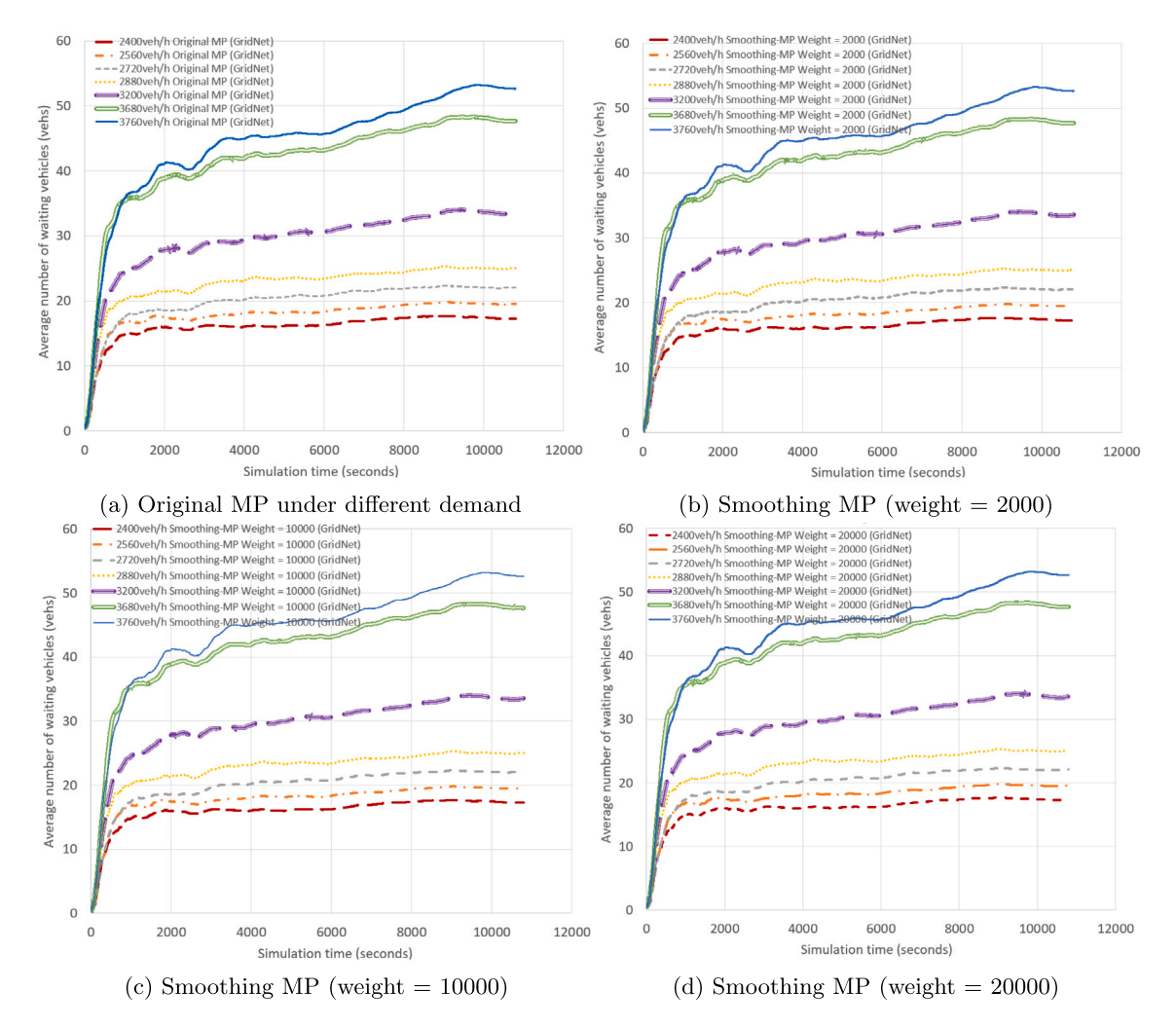


Fig. 3. Stability analysis (Grid Network).

Original MP control significantly exceeds that under the Smoothing-MP with varying weight values, as shown in Fig. 10(a). However, for the corridor's conflict direction in the Grid Network, the average delay under the Original MP control is lower than under the Smoothing-MP with different weight values for vehicle demands of 800, 1600, 2400, 3200, and 3760 vehicles per hour. When vehicle demand equals 3680 and 3840 vehicles per hour, the average delay for both Original MP and Smoothing-MP is comparably high, possibly due to vehicle demand exceeding the stable demand region within the Grid Network. In such circumstances, the Grid Network becomes highly congested, leading to minimal differences between the two controllers along the conflict direction, as depicted in Fig. 10(b).

For the Austin Network, a similar pattern emerges, with the average delay under the Original MP control being considerably higher than that under the Smoothing-MP along the signal coordinated corridor direction, as depicted in Fig. 12(a). Conversely, in the corridor conflict direction, the average delay under the Original MP control remains higher than under the Smoothing-MP control, as shown in Fig. 12(b). Overall, both the Grid Network and the Austin Network exhibit analogous patterns concerning the metric of average delay.

For a more comprehensive understanding, we evaluated the average delay experienced by each vehicle traveling in the direction of signal coordination as well as in the conflicting direction for both the Grid Network and the Austin Network. The results are presented in Figs. 11 and 13. It is important to note that the average delay per vehicle is a metric evaluated at an individual vehicle level. The data presented in both figures indicate that the Smoothing-MP control system prioritizes the coordination direction, evidenced by reduced delays for the signal coordination corridor direction and increased delays for the signal coordination conflict direction.

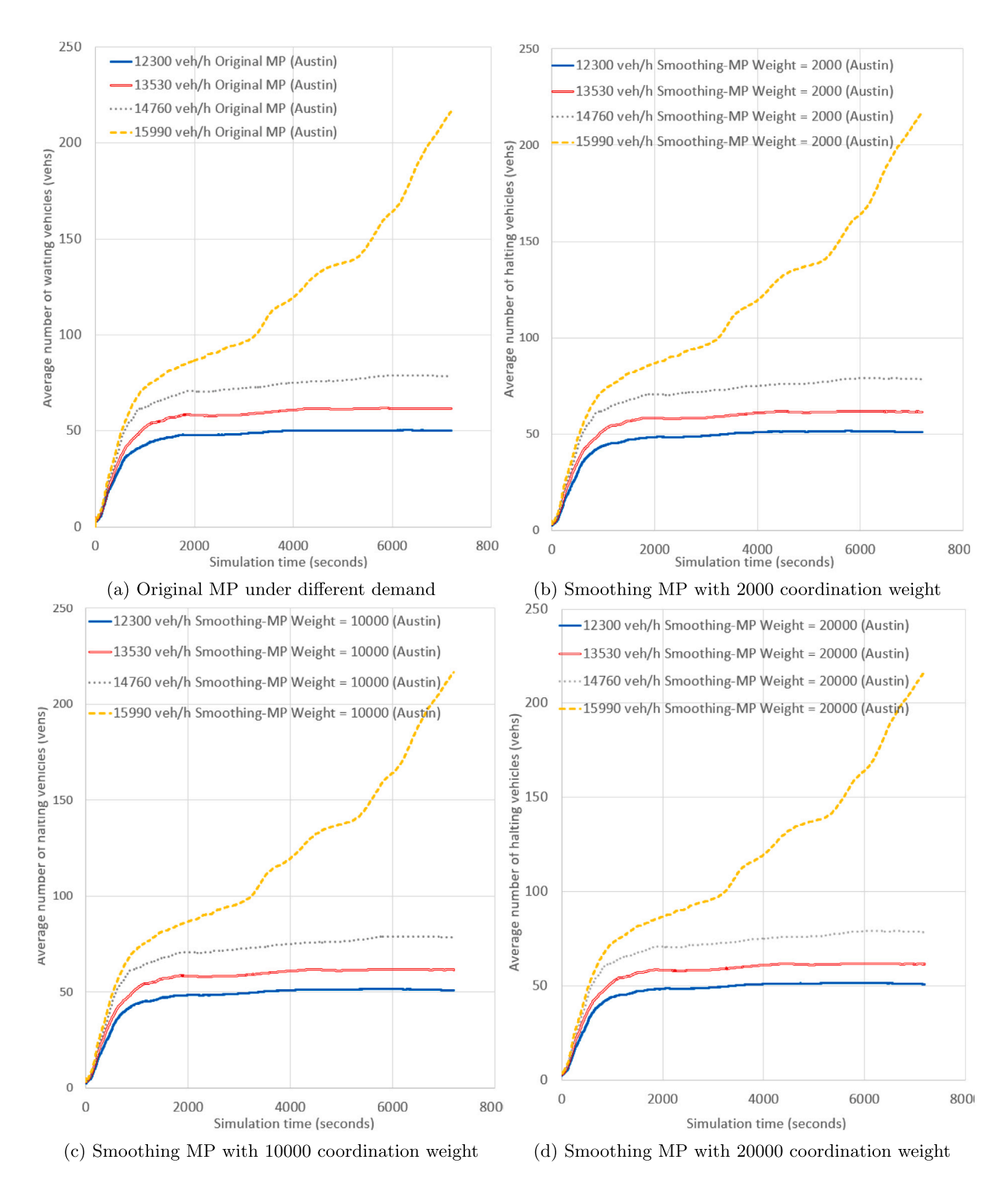


Fig. 4. Stability analysis (Austin Network)

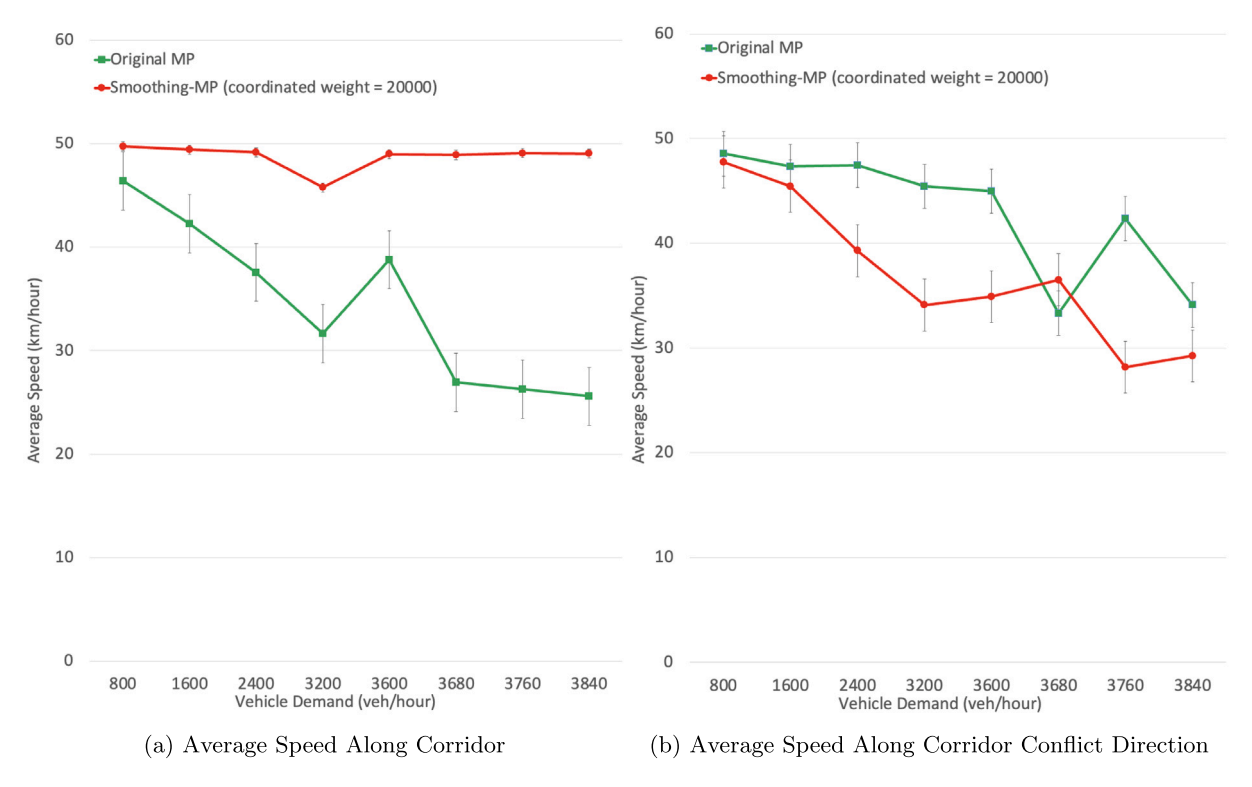


Fig. 5. Average speed comparison (Grid Network).

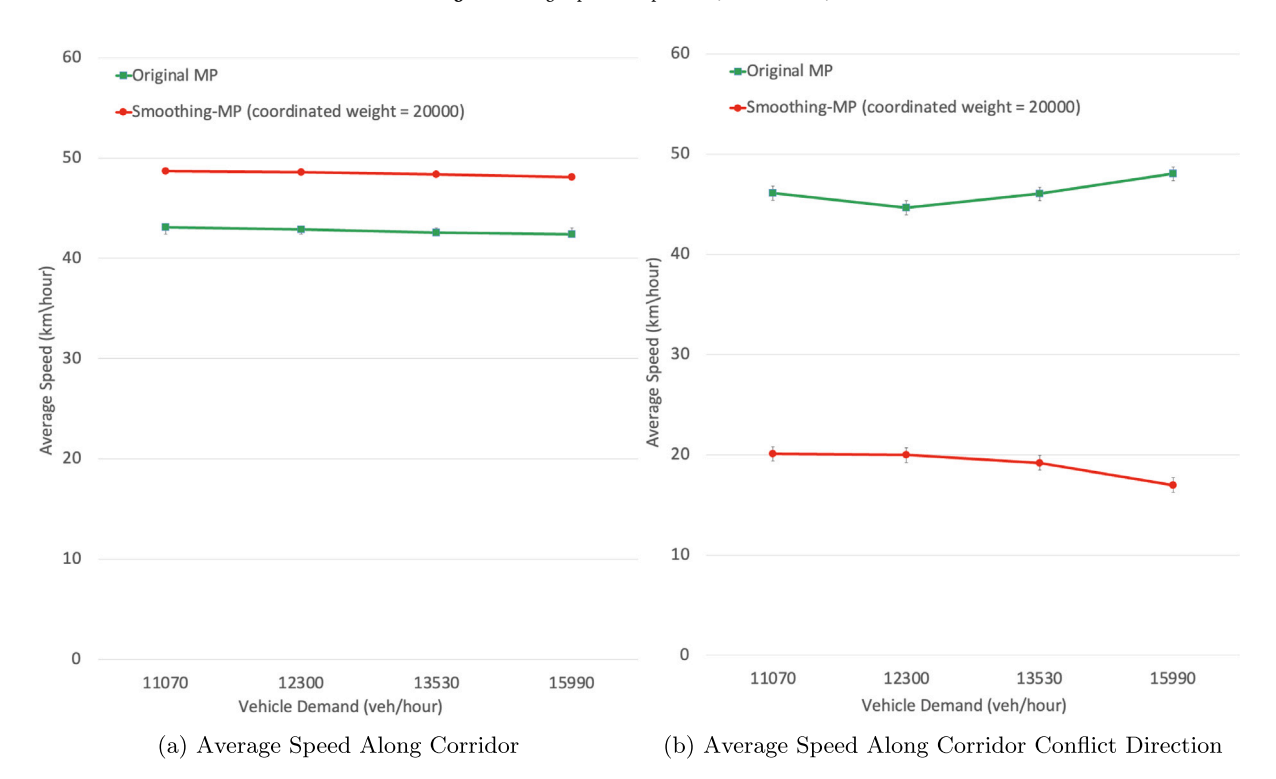


Fig. 6. Average speed comparison (Austin Network).

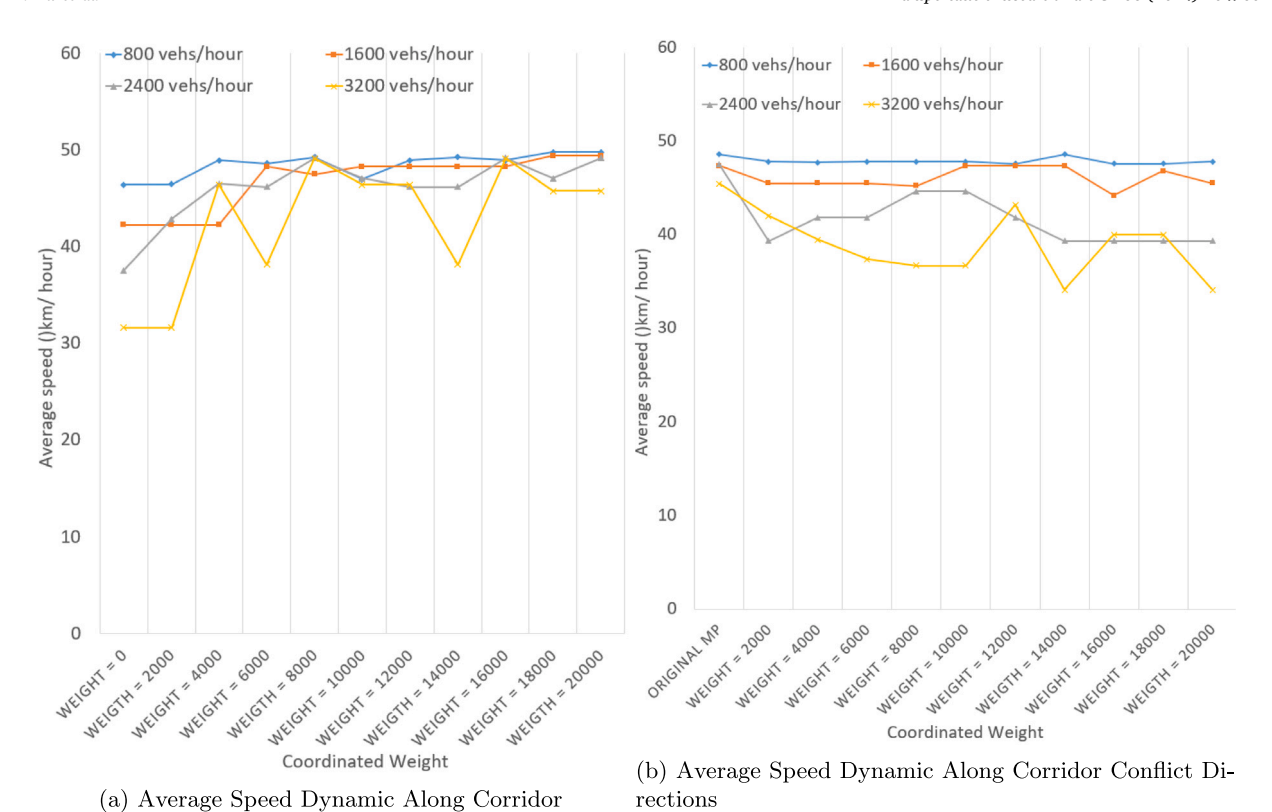


Fig. 7. Average speed dynamic comparison (Grid Network).

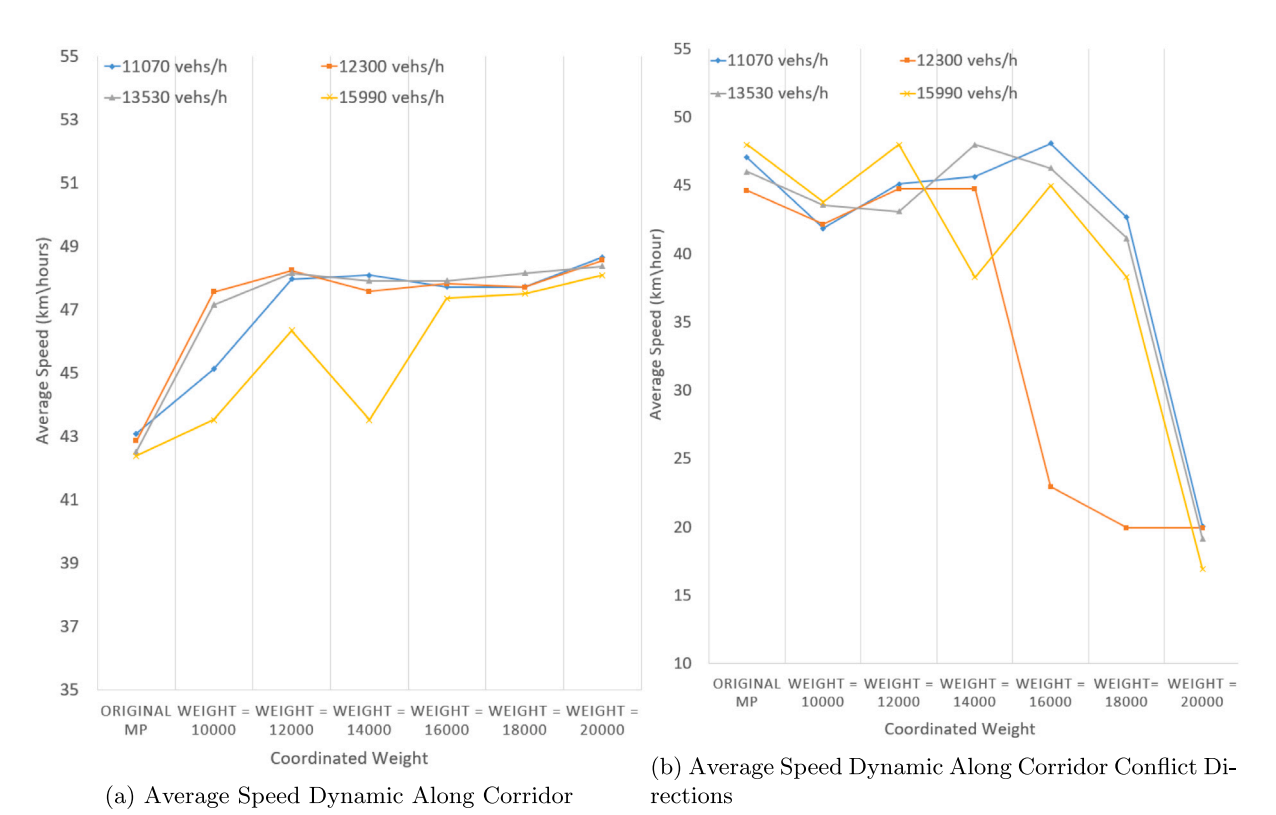


Fig. 8. Average speed dynamic comparison (Austin Network).

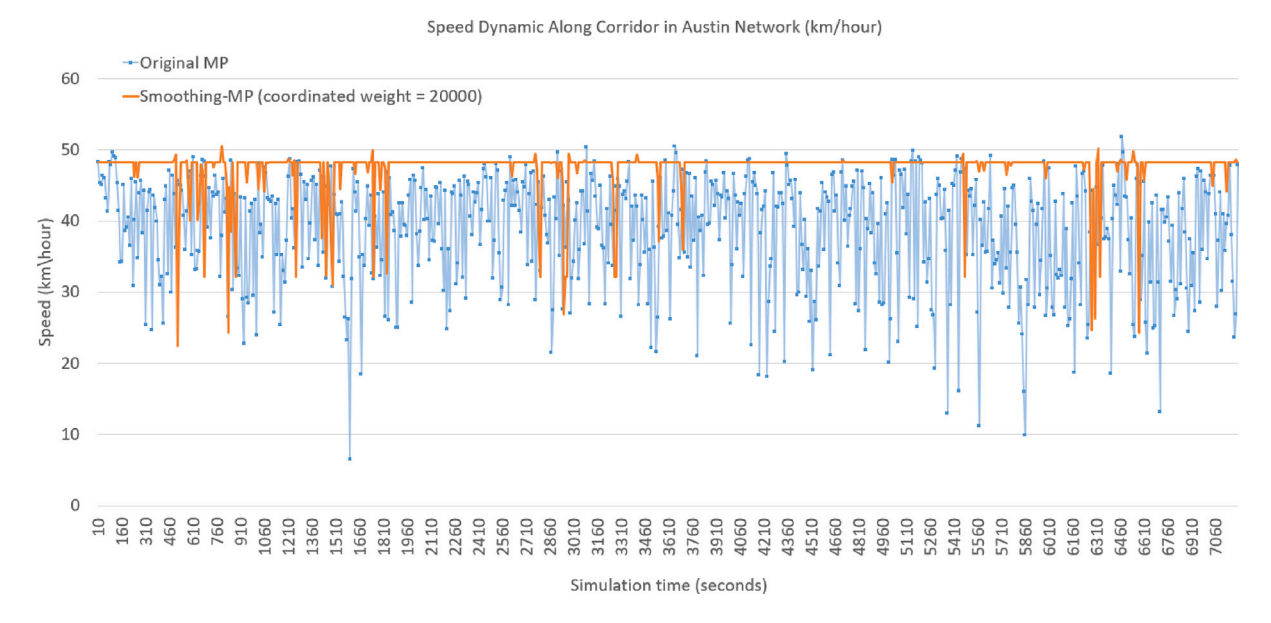


Fig. 9. Speed dynamics.

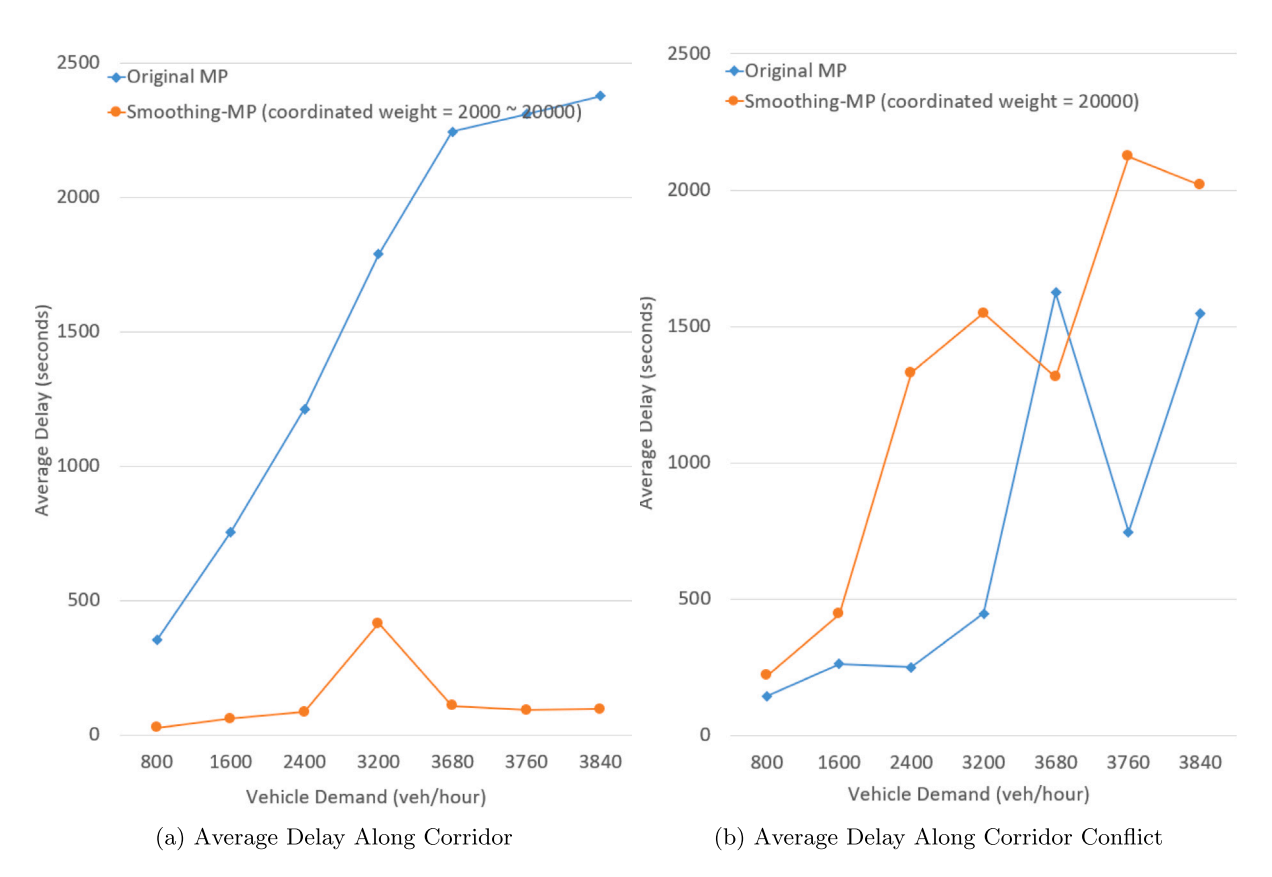


Fig. 10. Average delay comparison (Grid Network).

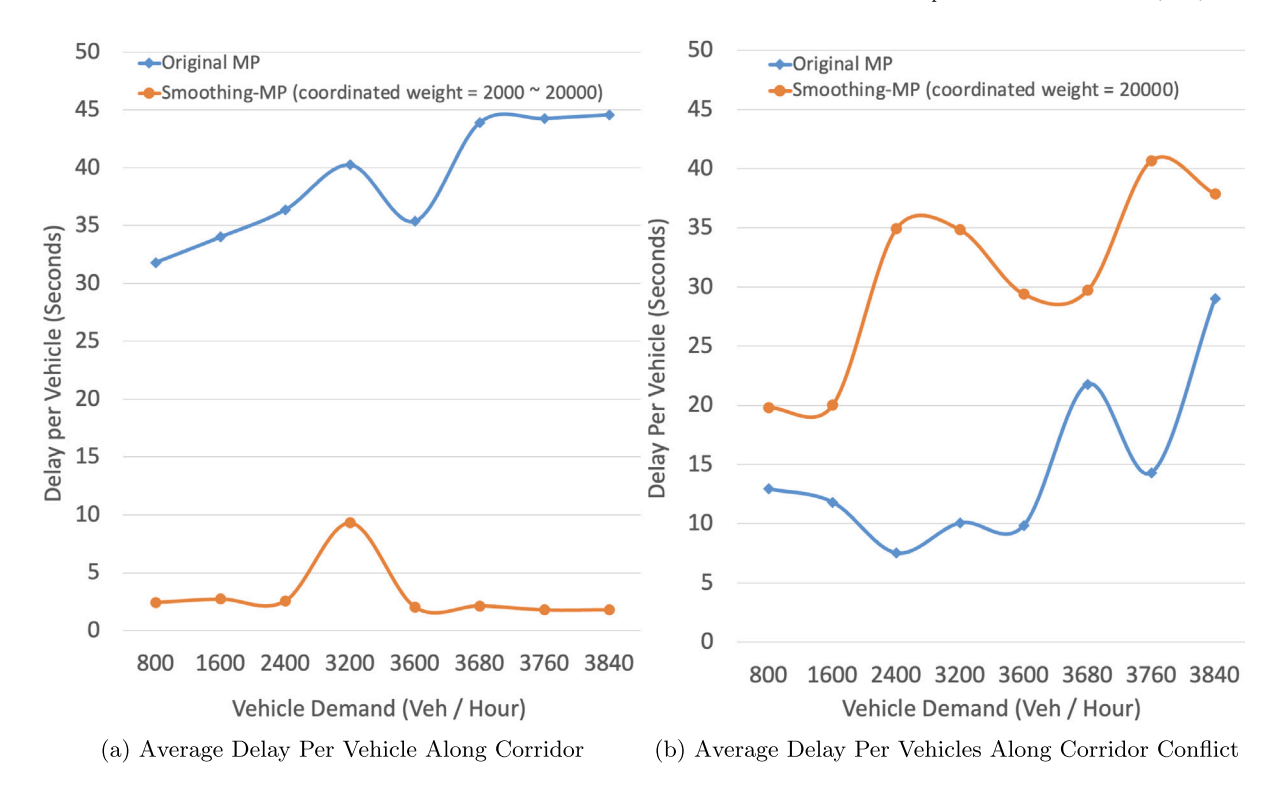


Fig. 11. Average delay per vehicle comparison (Grid Network).

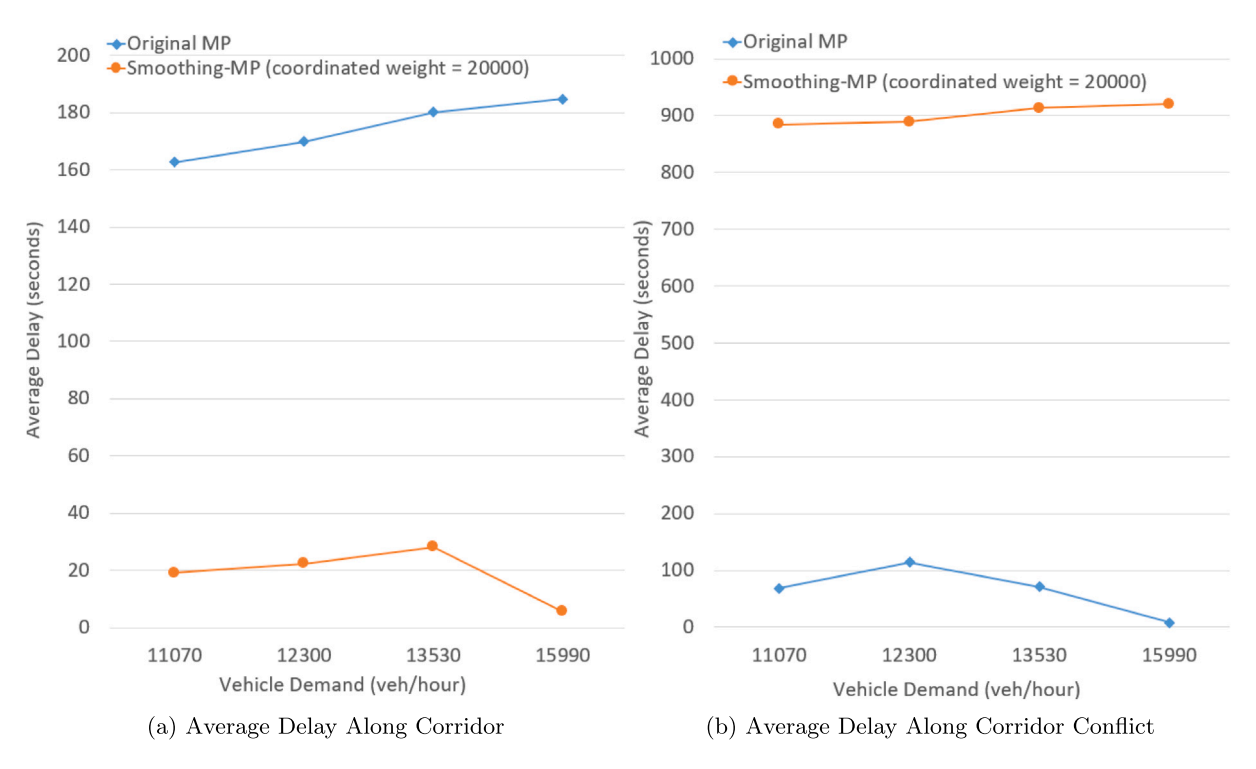


Fig. 12. Average delay comparison (Austin Network).

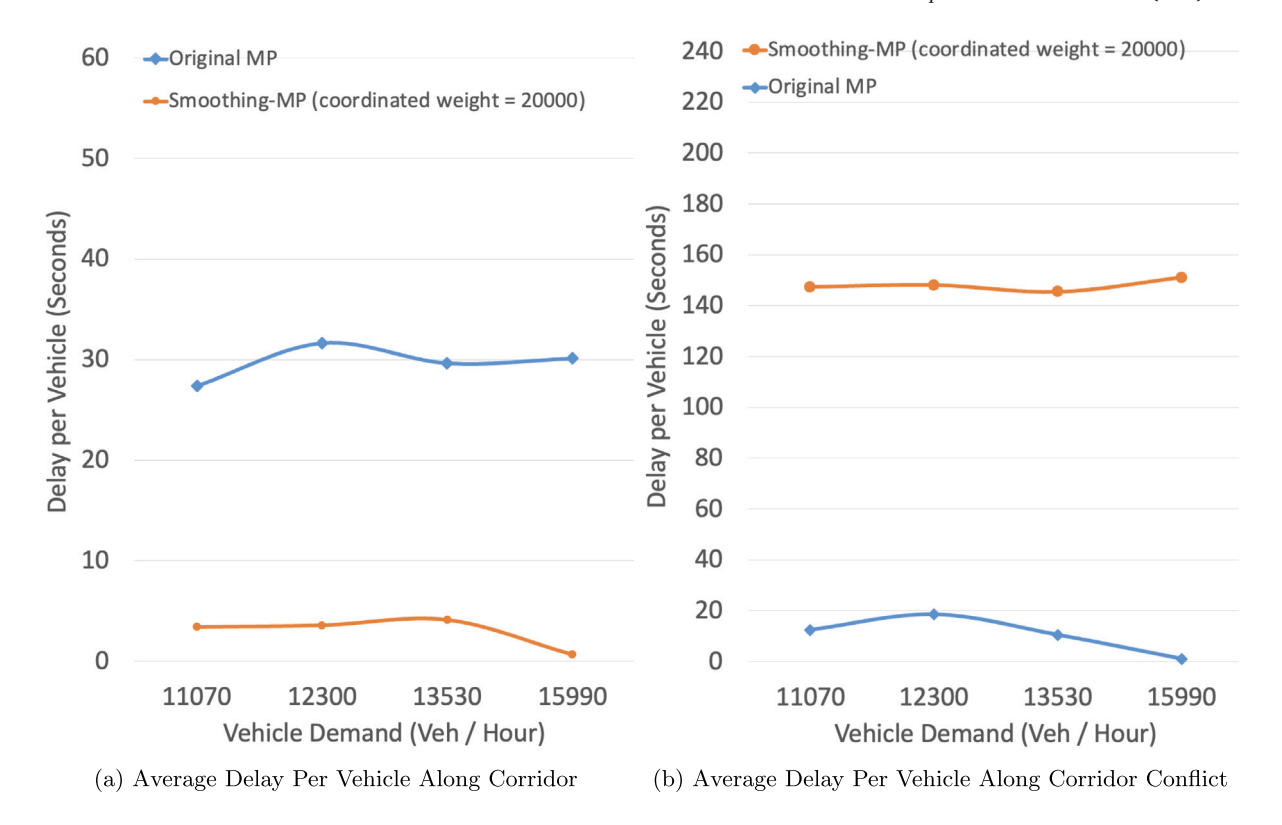


Fig. 13. Average delay per vehicle comparison (Austin Network).

# 5.4. Average fuel consumption

Fuel consumption is a pivotal metric in assessing the efficiency of signal control systems. In our study, we meticulously simulate fuel consumption for vehicles traversing specific corridors and their intersecting routes within both the Grid Network and the Austin Network, across various levels of vehicle demand. To achieve this, we employ the Passenger Car and Heavy-Duty Emission Model (PHEM), an advanced instantaneous vehicle emission model that has been developed for precision in emission factor estimation, as documented by Hausberger (2003). PHEM provides the foundation for the emission factors presented in the Handbook Emission Factors for Road Transport (HBEFA) (Notter et al., 2021).

Our model for fuel consumption is derived from a continuous model found within the HBEFA database, which meticulously considers variables such as vehicle speed, acceleration, and the specific engine technology at play. This nuanced approach is fully embraced and operationalized within the SUMO simulation environment, as highlighted in studies by Krajzewicz et al. (2012) and Salles et al. (2020). SUMO's capability to implement the pollutant emission model means that we can accurately track and record the emissions and fuel consumption data for each vehicle throughout its journey. Furthermore, SUMO enables the aggregation and recording of emissions data at the lane or edge level over specified time intervals, ensuring a detailed and comprehensive analysis of fuel consumption patterns (Krajzewicz et al., 2012).

An examination of both Figs. 14 and 16 elucidates a decline in vehicle fuel consumption corresponding to an increase in the signal coordination weight along the coordinated corridor directions, the unit is mg per second. In stark contrast, an increasing trend is noticeable as the signal coordination weight intensifies along the conflict directions of the signal coordination corridor, observed across different vehicular demand levels (see Figs. 15 and 17).

# 6. Conclusions

To our understanding, there exists a gap in current research in the integration of max-pressure (MP) signal timing with signal coordination. Addressing this, our study proposes a pioneering application of MP signal control, which incorporates signal coordination along the corridor for the first time, aimed at smoothing traffic. Moreover, we present a meticulous proof showcasing that our innovative Smoothing-MP approach can maintain maximum stability properties, even while introducing signal coordination. This fresh perspective has the potential to broaden the practical utility of MP control, particularly considering that real-world traffic seldom exhibits uniform distribution across the network.

Numerical results from both the Grid Network and the Downtown Austin Network suggest that the stable region remains unaffected after implementing Smoothing-MP compared to the Original MP control. Regarding corridor directions exhibit higher

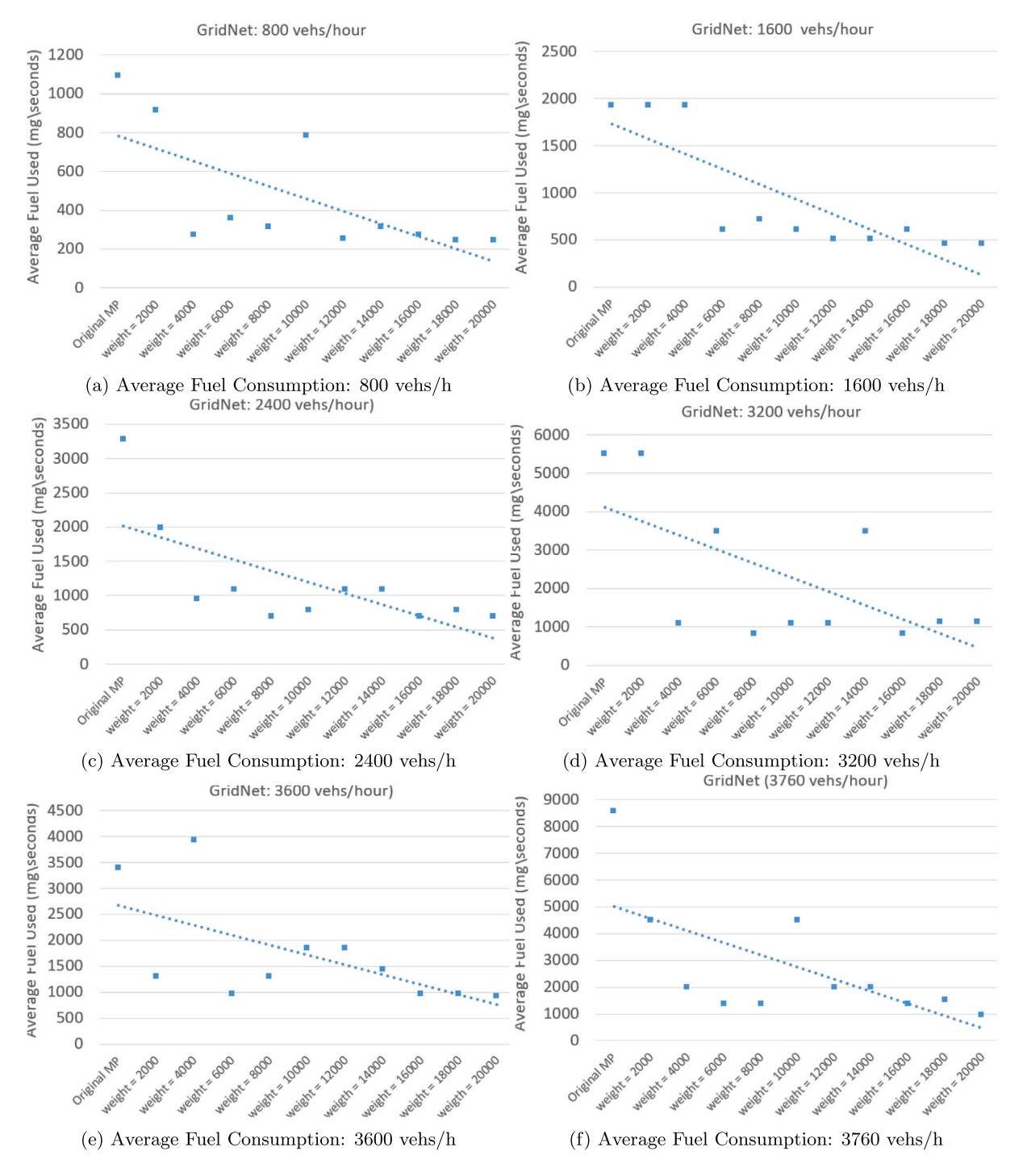


Fig. 14. Average fuel consumption analysis along corridor direction (Grid Network).

speeds under Smoothing-MP compared to the Original MP control, while the contrary is true for corridor conflict directions. Based on speed dynamics illustrated in Figs. 7(a) to 9, we deduce that higher signal coordination weights yield higher average speeds along corridors, while speed dynamics display a reversed pattern at corridor conflict directions. Regarding average delay, corridor directions experience lower average delays under Smoothing-MP compared to the Original MP control, whereas corridor conflict directions register higher average speeds under Smoothing-MP compared to the Original MP control.

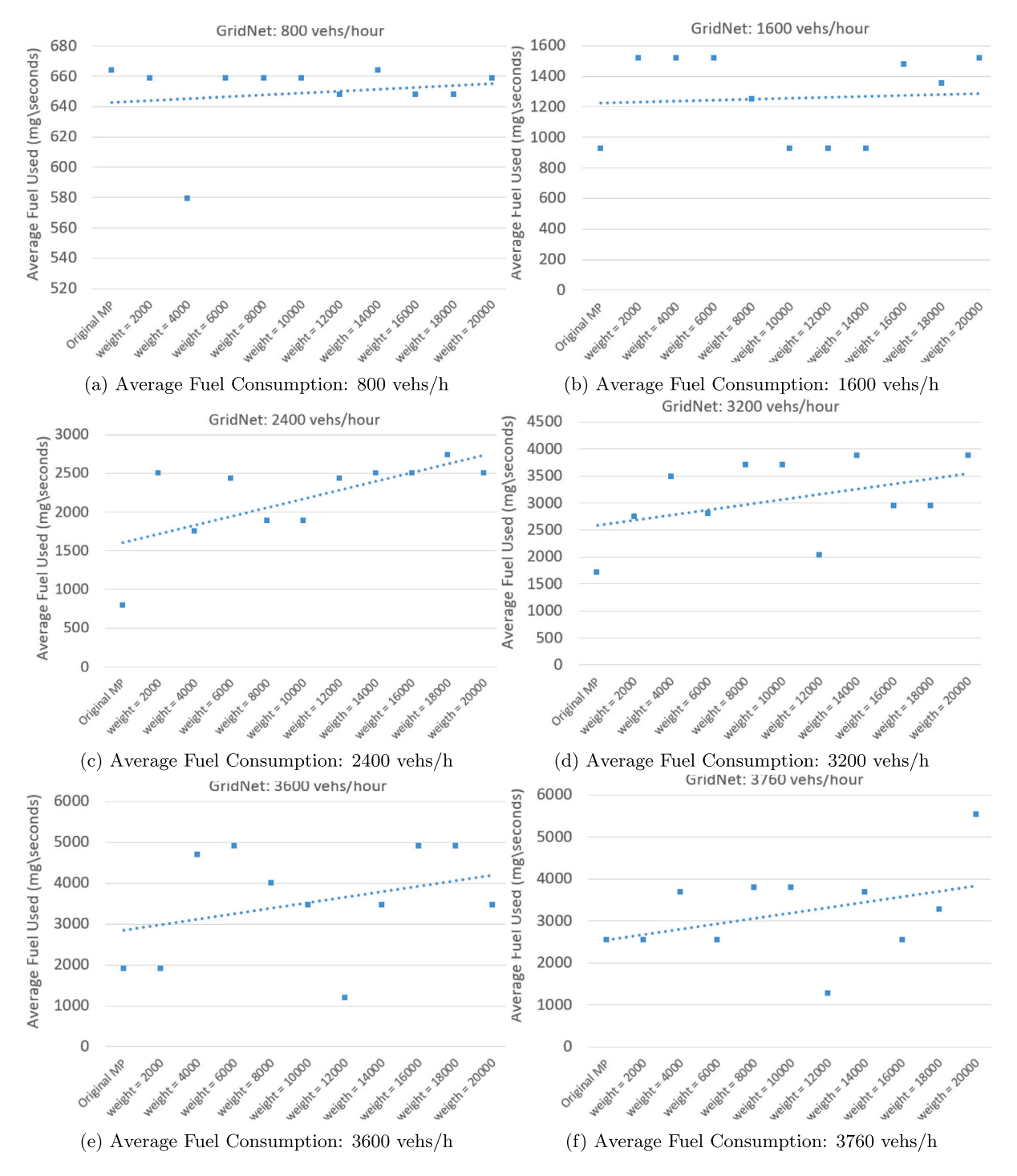


Fig. 15. Average fuel consumption analysis corridor conflict direction (Grid Network).

Both sets of results indicate that Smoothing-MP prioritizes signal coordination direction over conflict directions. The higher the weight, the greater the level of priority. However, the network-level average number of waiting vehicles and average travel time remain consistent, regardless of the consideration of signal coordination.

Future work includes numerous potential extensions. For instance, integrating Connected and Autonomous Vehicles (CAVs) into the Smoothing-MP control could provide more accurate speed and travel time information, thereby improving signal timing. Another

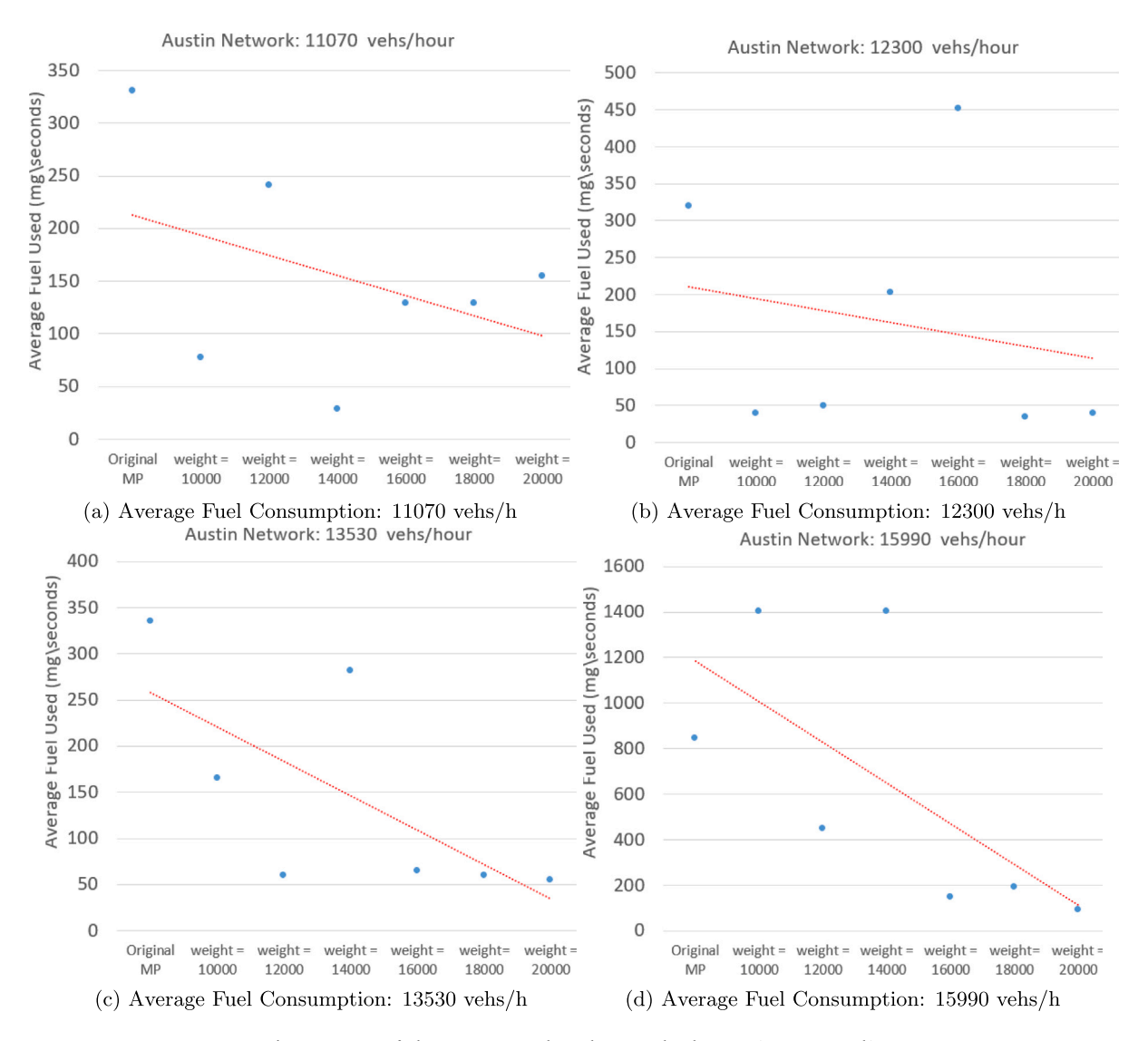


Fig. 16. Average fuel consumption analysis along corridor direction (Austin Network).

intriguing challenge and topic for future study would be the integration of multimodal traffic and signal coordination within the MP control framework.

# CRediT authorship contribution statement

**Te Xu:** Conceptualization, Investigation, Methodology, Software, Validation, Visualization, Writing – original draft, Writing – review & editing. **Simanta Barman:** Software, Validation. **Michael W. Levin:** Conceptualization, Funding acquisition, Methodology, Resources, Supervision, Validation, Writing – original draft, Writing – review & editing.

### Acknowledgments

The authors gratefully acknowledge the support of the National Science Foundation, United States, Award No. 1935514 and the support of Hsiao Shaw-Lundquist Fellowship of the University of Minnesota China Center.

All authors reviewed the results and approved the final version of the manuscript.

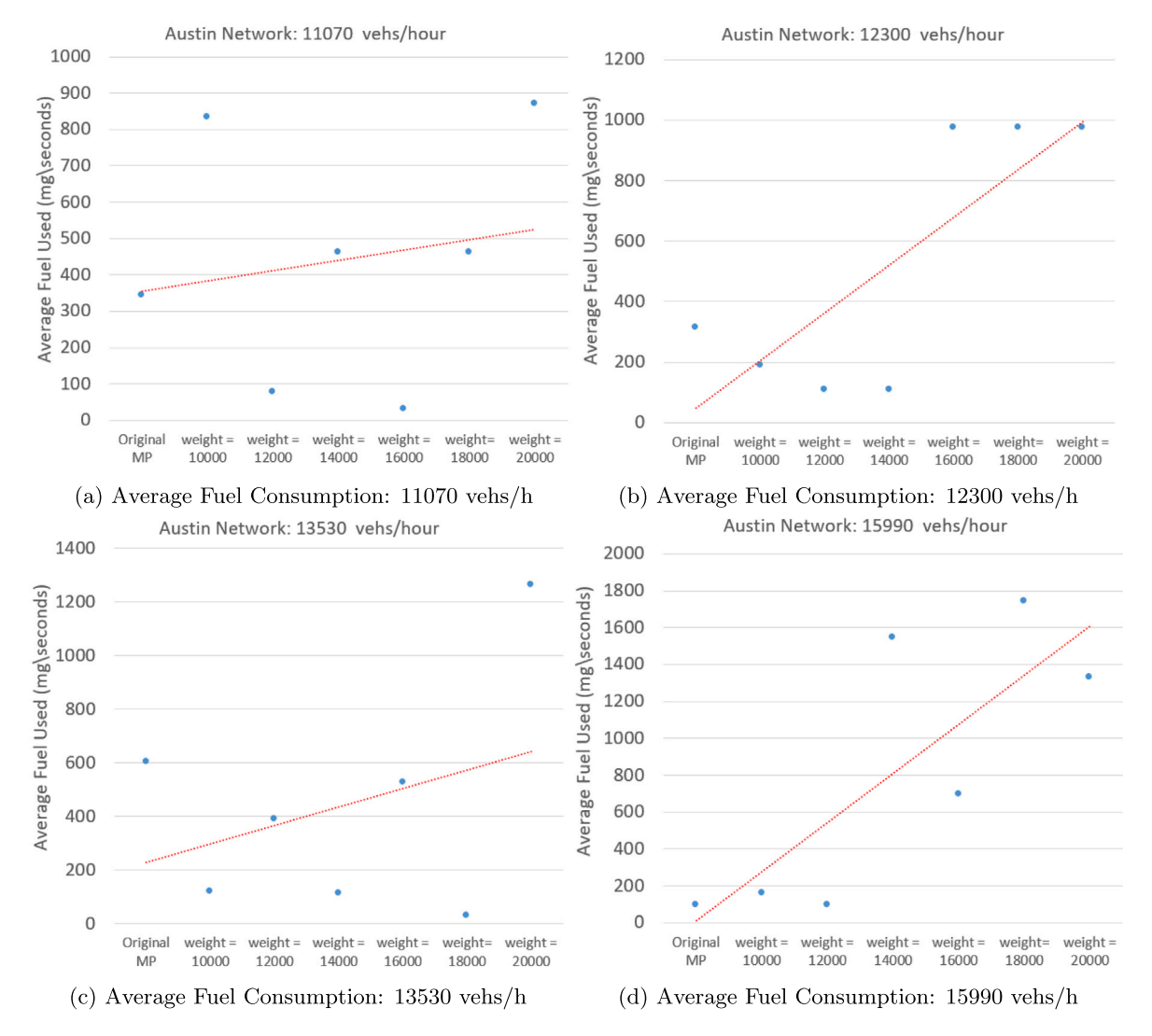


Fig. 17. Average fuel consumption analysis corridor conflict direction (Austin Network).

#### References

Anderson, L., Pumir, T., Triantafyllos, D., Bayen, A.M., 2018. Stability and implementation of a cycle-based max pressure controller for signalized traffic networks. Netw. Heterog. Media 13 (2), 241.

Arsava, T., Xie, Y., Gartner, N., 2018. OD-NETBAND: An approach for origin-destination based network progression band optimization. Transp. Res. Rec. 2672 (18), 58-70.

Barman, S., Levin, M.W., 2022. Performance evaluation of modified cyclic max-pressure controlled intersections in realistic corridors. Transp. Res. Rec. 03611981211072807.

Barman, S., Levin, M.W., 2023. Throughput properties and optimal locations for limited deployment of max-pressure controls. Transp. Res. C 150, 104105. Boukerche, A., Zhong, D., Sun, P., 2021. A novel reinforcement learning-based cooperative traffic signal system through max-pressure control. IEEE Trans. Veh.

Chang, W., Roy, D., Zhao, S., Annaswamy, A., Chakraborty, S., 2020. CPS-oriented modeling and control of traffic signals using adaptive back pressure. In: 2020 Design, Automation & Test in Europe Conference & Exhibition. DATE, IEEE, pp. 1686–1691.

Chen, R., 2021. Maximum-stability Distributed Control in Traffic Networks (Ph.D. thesis). University of Minnesota.

Das, D., Altekar, N.V., Head, K.L., 2022. Priority-based traffic signal coordination system with multi-modal priority and vehicle actuation in a connected vehicle environment. Transp. Res. Rec. 03611981221134627.

de Oliveira, M.G.S., Ribeiro, P.C.M., 2001. Production and analysis of coordination plans using a geographic information system. Transp. Res. C 9 (1), 53–68. Dixit, V., Nair, D.J., Chand, S., Levin, M.W., 2020. A simple crowdsourced delay-based traffic signal control. PLoS One 15 (4), e0230598.

Fagnant, D.J., Kockelman, K., 2015. Preparing a nation for autonomous vehicles: Opportunities, barriers and policy recommendations. Transp. Res. A 77, 167–181. Feng, Y., 2015. Intelligent Traffic Control in a Connected Vehicle Environment (Ph.D. thesis). The University of Arizona.

Gartner, N.H., Assman, S.F., Lasaga, F., Hou, D.L., 1991. A multi-band approach to arterial traffic signal optimization. Transp. Res. B 25 (1), 55–74.

Girault, J.-T., Gayah, V.V., Guler, I., Menendez, M., 2016. Exploratory analysis of signal coordination impacts on macroscopic fundamental diagram. Transp. Res. Rec. 2560 (1), 36–46.

- Gregoire, J., Frazzoli, E., de La Fortelle, A., Wongpiromsarn, T., 2014. Back-pressure traffic signal control with unknown routing rates. IFAC Proc. Vol. 47 (3), 11332–11337.
- Guo, Q., Li, L., Ban, X.J., 2019. Urban traffic signal control with connected and automated vehicles: A survey. Transp. Res. C 101, 313-334.

Hausberger, S., 2003. Simulation of real world vehicle exhaust emission.

- Hu, H., Liu, H.X., 2013. Arterial offset optimization using archived high-resolution traffic signal data. Transp. Res. C 37, 131-144.
- Krajzewicz, D., Erdmann, J., Behrisch, M., Bieker, L., 2012. Recent development and applications of SUMO-simulation of urban mobility. Int. J. Adv. Syst. Measur. 5 (3&4).
- Le, T., Kovács, P., Walton, N., Vu, H.L., Andrew, L.L., Hoogendoorn, S.S., 2015. Decentralized signal control for urban road networks. Transp. Res. C 58, 431–450. Levin, M.W., 2022. A general maximum-stability dispatch policy for shared autonomous vehicle dispatch with an analytical characterization of the maximum throughput. Transp. Res. B 163, 258–280.
- Levin, M.W., Hu, J., Odell, M., 2020. Max-pressure signal control with cyclical phase structure. Transp. Res. C 120, 102828.
- Li, L., Jabari, S.E., 2019. Position weighted backpressure intersection control for urban networks. Transp. Res. B 128, 435-461.
- Li, T., Klavins, J., Xu, T., Zafri, N.M., Stern, R., 2023. Understanding driver-pedestrian interactions to predict driver yielding: Naturalistic open-source dataset collected in minnesota. arXiv preprint arXiv:2312.15113.
- Little, J.D., Kelson, M.D., Gartner, N.H., 1981. MAXBAND: A Versatile Program for Setting Signals on Arteries and Triangular Networks. Alfred P. Sloan School of Management, Massachusetts Institute of Technology.
- Liu, H., Gayah, V.V., 2022. A novel max pressure algorithm based on traffic delay. arXiv preprint arXiv:2202.03290.
- Liu, J., Zhang, H., Fu, Z., Wang, Y., 2021. Learning scalable multi-agent coordination by spatial differentiation for traffic signal control. Eng. Appl. Artif. Intell. 100, 104165
- Lopez, P.A., Behrisch, M., Bieker-Walz, L., Erdmann, J., Flötteröd, Y.-P., Hilbrich, R., Lücken, L., Rummel, J., Wagner, P., ner, E.W., 2018. Microscopic traffic simulation using SUMO. In: The 21st IEEE International Conference on Intelligent Transportation Systems. IEEE, URL https://elib.dlr.de/124092/.
- Lv, J., Zhang, Y., 2012. Effect of signal coordination on traffic emission. Transp. Res. D 17 (2), 149-153.
- Ma, W., An, K., Lo, H.K., 2016. Multi-stage stochastic program to optimize signal timings under coordinated adaptive control. Transp. Res. C 72, 342-359.
- Ma, W., Cheng, R., Ke, H., Zhang, J., 2018a. Store-brand production arrangement based on the game theory. Math. Probl. Eng. 2018.
- Ma, D., Xiao, J., Song, X., Ma, X., Jin, S., 2020. A back-pressure-based model with fixed phase sequences for traffic signal optimization under oversaturated networks. IEEE Trans. Intell. Transp. Syst. 22 (9), 5577–5588.
- Ma, W., Zou, L., An, K., Gartner, N.H., Wang, M., 2018b. A partition-enabled multi-mode band approach to arterial traffic signal optimization. IEEE Trans. Intell. Transp. Syst. 20 (1), 313–322.
- Maipradit, A., Kawakami, T., Liu, Y., Gao, J., Ito, M., 2021. An adaptive traffic signal control scheme based on back-pressure with global information. J. Inf. Process. 29, 124–131.
- Mercader, P., Uwayid, W., Haddad, J., 2020. Max-pressure traffic controller based on travel times: An experimental analysis. Transp. Res. C 110, 275–290.

National Academies of Sciences, Engineering, and Medicine, et al., 2015. Signal Timing Manual.

- Noaeen, M., Mohajerpoor, R., Far, B.H., Ramezani, M., 2021. Real-time decentralized traffic signal control for congested urban networks considering queue spillbacks. Transp. Res. C 133, 103407.
- Notter, B., Hausberger, S., Matzer, C.U., Weller, K., Dippold, M., Politschnig, N., Lipp, S., 2021. HBEFA 4.2-Documentation of updates.
- Pian, W., Wu, Y., Qu, X., Cai, J., Kou, Z., 2020. Spatial-temporal dynamic graph attention networks for ride-hailing demand prediction. arXiv preprint arXiv:2006.05905.
- Qi, H., Dai, R., Tang, Q., Hu, X., 2020. Coordinated intersection signal design for mixed traffic flow of human-driven and connected and autonomous vehicles. IEEE Access 8, 26067–26084.
- Rey, D., Levin, M.W., 2019. Blue phase: Optimal network traffic control for legacy and autonomous vehicles. Transp. Res. B 130, 105-129.
- Robbennolt, J., Levin, M.W., 2023. Maximum throughput dispatch for shared autonomous vehicles including vehicle rebalancing. IEEE Trans. Intell. Transp. Syst. 24 (9), 9871–9885.
- Robertson, D.I., 1969. TRANSYT: A traffic network study tool.
- Salles, D., Kaufmann, S., Reuss, H.-C., 2020. Extending the intelligent driver model in SUMO and verifying the drive off trajectories with aerial measurements. In: SUMO Conference Proceedings, vol. 1, pp. 1–25.
- Smith, M.J., Iryo, T., Mounce, R., Rinaldi, M., Viti, F., 2019. Traffic control which maximises network throughput: Some simple examples. Transp. Res. C 107, 211–228.
- Su, Z., Chow, A.H., Zhong, R., 2021. Adaptive network traffic control with an integrated model-based and data-driven approach and a decentralised solution method. Transp. Res. C 128, 103154.
- Sun, X., Yin, Y., 2018. A simulation study on max pressure control of signalized intersections. Transp. Res. Rec. 2672 (18), 117-127.
- Taale, H., van Kampen, J., Hoogendoorn, S., 2015. Integrated signal control and route guidance based on back-pressure principles. Transp. Res. Procedia 10, 226–235.
- Tassiulas, L., Ephremides, A., 1990. Stability properties of constrained queueing systems and scheduling policies for maximum throughput in multihop radio networks. In: 29th IEEE Conference on Decision and Control. IEEE, pp. 2130–2132.
- Varaiya, P., 2013. Max pressure control of a network of signalized intersections. Transp. Res. C 36, 177-195.
- Vickrey, W.S., 1969. Congestion theory and transport investment. Am. Econ. Rev. 59 (2), 251-260.
- Wang, X., Yin, Y., Feng, Y., Liu, H.X., 2022. Learning the max pressure control for urban traffic networks considering the phase switching loss. Transp. Res. C 140, 103670.
- Webster, F.V., 1958. Traffic Signal Settings. Technical Report.
- Wei, H., Chen, C., Zheng, G., Wu, K., Gayah, V., Xu, K., Li, Z., 2019. Presslight: Learning max pressure control to coordinate traffic signals in arterial network. In: Proceedings of the 25th ACM SIGKDD International Conference on Knowledge Discovery & Data Mining. pp. 1290–1298.
- Wei, H., Zheng, G., Gayah, V., Li, Z., 2021. Recent advances in reinforcement learning for traffic signal control: A survey of models and evaluation. ACM SIGKDD Explor. Newsl. 22 (2), 12–18.
- Wong, S., Wong, W., Leung, C., Tong, C., 2002. Group-based optimization of a time-dependent TRANSYT traffic model for area traffic control. Transp. Res. B 36 (4), 291–312.
- Xiao, N., Frazzoli, E., Li, Y., Luo, Y., Wang, Y., Wang, D., 2015a. Further study on extended back-pressure traffic signal control algorithm. In: 2015 54th IEEE Conference on Decision and Control. CDC, IEEE, pp. 2169–2174.
- Xiao, N., Frazzoli, E., Luo, Y., Li, Y., Wang, Y., Wang, D., 2015b. Throughput optimality of extended back-pressure traffic signal control algorithm. In: 2015 23rd Mediterranean Conference on Control and Automation. MED, IEEE, pp. 1059–1064.
- Xu, T., 2023. Boosting Max-Pressure Signal Control into Practical Implementation: Methodologies and Simulation Studies in City Networks (Ph.D. thesis). University of Minnesota.
- Xu, T., Barman, S., Levin, M.W., Chen, R., Li, T., 2022a. Integrating public transit signal priority into max-pressure signal control: Methodology and simulation study on a downtown network. Transp. Res. C 138, 103614.
- Xu, T., Bika, Y., Levin, M., 2022b. An approximate position-weighted back-pressure traffic signal control policy for traffic networks, Available at SSRN 4186584.

- Xu, T., Bika, Y., Levin, M.W., 2024a. Ped-MP: A pedestrian-friendly max-pressure signal control policy for city networks. J. Transport. Eng. A: Syst. 150 (7), 04024028.
- Xu, T., Cieniawski, M., Levin, M.W., 2024b. FMS-dispatch: A fast maximum stability dispatch policy for shared autonomous vehicles including exiting passengers under stochastic travel demand. Transportmetrica A: Transp. Sci. 20 (3), 2214968.
- Xu, T., Levin, M.W., Cieniawski, M., 2021. A zone-based dynamic queueing model and maximum-stability dispatch policy for shared autonomous vehicles. In: 2021 IEEE International Intelligent Transportation Systems Conference. ITSC, IEEE, pp. 3827–3832.
- Yan, H., He, F., Lin, X., Yu, J., Li, M., Wang, Y., 2019. Network-level multiband signal coordination scheme based on vehicle trajectory data. Transp. Res. C 107, 266–286.
- Yao, J., Tan, C., Tang, K., 2019. An optimization model for arterial coordination control based on sampled vehicle trajectories: The STREAM model. Transport. Res. C 109, 211–232.
- Yu, H., Liu, P., Fan, Y., Zhang, G., 2021. Developing a decentralized signal control strategy considering link storage capacity. Transp. Res. C 124, 102971.
- Yue, R., 2020. Determination of Progression Speeds for Traffic Signal Coordination (Ph.D. thesis). University of Nevada, Reno.
- Zaidi, A., Kulcsár, B., Wymeersch, H., 2016. Decentralized traffic signal control with fixed and adaptive routing of vehicles in urban road networks. IEEE Trans. Intell. Transport. Syst. 17 (8), 2134–2143.
- Zhang, H., Nie, Y., Qian, Z., 2013. Modelling network flow with and without link interactions: the cases of point queue, spatial queue and cell transmission model. Transportmetrica B 1 (1), 33–51.
- Zhang, L., Song, Z., Tang, X., Wang, D., 2016. Signal coordination models for long arterials and grid networks. Transp. Res. C 71, 215-230.
- Zhang, C., Xie, Y., Gartner, N.H., Stamatiadis, C., Arsava, T., 2015. AM-band: An asymmetrical multi-band model for arterial traffic signal coordination. Transp. Res. C 58, 515–531.
- Zhang, Y., Zhou, Y., 2018. Distributed coordination control of traffic network flow using adaptive genetic algorithm based on cloud computing. J. Netw. Comput. Appl. 119, 110–120.
- Zhou, S., Li, H., Zhang, Q., Gao, M., Ran, B., 2021. Traffic signal coordination control optimization considering vehicle emissions on urban arterial road. J. Comput. Methods Sci. Eng. 21 (1), 233–239.